Theory of multiphoton single and double ionization of two-electron atomic systems driven by short-wavelength electric fields: An *ab initio* treatment

Emmanuel Foumouo,[1] Gérard Lagmago Kamta,[2] Gaston Edah,[3] and Bernard Piraux[1]
[1]*Laboratoire de Physique Atomique, Moléculaire et Optique (unité PAMO), Université Catholique de Louvain, 2, chemin du Cyclotron, B-1348 Louvain-la-Neuve, Belgium*
[2]*Department of Chemistry, University of Sherbrooke, 2500, Boulevard de l'Université, Sherbrooke, Québec, J1 K 2R1, Canada*
[3]*Institut de Mathématiques et de Sciences Physiques, 01 BP 613, Porto-Novo, Benin*
(Received 28 June 2006; revised manuscript received 21 September 2006; published 15 December 2006)

We give a detailed account of an *ab initio* computational treatment of multiphoton single ionization (with or without excitation) as well as double ionization of two-electron atoms exposed to short-wavelength electric fields. This treatment is time dependent and based on a spectral method of configuration interaction type combined with Jacobi or *J*-matrix calculations. It involves a complete treatment of electron-electron correlation in the initial and final states as well as during the time propagation. The atom eigenvalue problem is first solved by means of the spectral method. It consists of expanding the atom wave function in a basis of products of complex Coulomb-Sturmian functions of the electron radial coordinates and bipolar harmonics of the angular coordinates. This method allows a high-resolution study of many atomic states, in particular high-lying singly excited states as well as many doubly excited states. Results for He are presented and discussed in detail. The time-dependent Schrödinger equation is then solved by means of an explicit scheme of Runge-Kutta type. An accurate calculation of the probability of single and double ionization is carried out by projecting the ionizing wave packet on fully correlated multichannel scattering wave functions generated by means of the *J*-matrix method. After a detailed analysis of the accuracy of this method, we show that our results for the total cross section of one-photon single and double ionization of He and H^- are in very good agreement with those obtained by the most sophisticated approaches. Two-photon double ionization of He is then considered, and results are presented in a frequency regime where substantial discrepancies subsist between all existing calculations. Our results demonstrate that electron correlations in the final state play a significant role.

DOI: 10.1103/PhysRevA.74.063409 PACS number(s): 32.80.Rm, 32.80.Fb, 42.50.Hz

I. INTRODUCTION

The study of the quantum dynamics of strongly correlated two-electron atomic systems driven by short-wavelength oscillating fields is a fundamental problem in atomic physics and a challenge for both experiment and theory. So far, most of the experimental works have focused on one-photon single ionization (SI) with excitation of the residual ion [1] as well as one-photon direct double ionization (DI) of two-active-electron atoms [2] by means of synchrotron light sources at x-ray wavelengths. Partial photoionization cross sections of He with both n and l final-ion-state separation have been measured recently by using lifetime-resolved fluorescence spectroscopy [3]. In the case of one-photon DI of He, absolute measurements of energies and angles of emission of the two strongly correlated photoelectrons [4] have provided a crucial test of the theoretical methods. At present, substantial efforts regarding the development of new XUV sources are made in two distinct directions. First, the generation of ultrashort pulses whose duration is close to the time scale associated with the electron-electron correlation in atoms: namely, attosecond pulses [5]. Second, the development of free-electron lasers operating at unprecedently high peak intensities in the far-x-ray regime [6]. These developments have opened the route to the study of the multiphoton single and double ionization (or excitation) of atoms at high frequency and intensity. Moving beyond the single-photon process introduces experimental complications related to the weakness of the signals. However, it also leads to a rich variety of new processes enabling a deeper exploration of electronic correlations [7].

SI with excitation of the residual ion and direct DI of atoms are processes where electron-electron correlation plays a dominant role. In the case of the one-photon transitions, SI with excitation and direct DI result from the electronic correlation. The theory of such processes requires, in principle, knowledge of the boundary conditions for the three-body partial and complete fragmentation of the system. This problem—in particular, the one related to the complete fragmentation of the atomic system—has been recognized as very challenging since the early contributions of Rudge, Seaton, and Peterkop [8]. One-photon direct DI of He has been studied by many authors after the pioneer work of Byron and Joachain [9]. However, it is only over the last decade that various nonperturbative approaches have been able to provide accurate data for both total and differential one-photon DI cross sections.

Brauner, Briggs, and Klar [10] derived an ansatz wave function which accounts for the three-body Coulomb interaction in the asymptotic region. This function, which we refer to as the BBK wave function, has been used by Maulbetsch and Briggs to obtain the angular distribution of the two photoelectrons in the case of He [11]. The results are in relatively good agreement in shape but not in amplitude with the experimental or other theoretical data [12]. A multichannel double-continuum wave function has been generated fully numerically by Nikolopoulos and Lambropoulos [7] within the framework of discretized bases involving linear

combinations of B splines. This wave function has been used in the calculation of the total cross section of one- as well as two-photon SI and DI of He.

Proulx and Shakeshaft [13] developed a sophisticated approach based on an expression for the total flux passing through a hypersphere of very large radius. Boundary conditions are incorporated within the stationary phase limit. Later on, Pont and Shakeshaft [14] reformulated this approach and managed to circumvent the problem of the asymptotic conditions by invoking projection operators: double ionization is separated from single ionization by projecting out the bound states of the one-electron ion (or atom) left behind after single ionization. These methods which require complex scaling of the total Hamiltonian have been generalized, at least formally, to treat multiphoton transitions [15]. However, to date, accurate results for total and differential cross sections have been obtained only in the case of one-photon DI of He. The first systematic study of the DI and SI with excitation of the He isoelectronic sequence was carried out by Kheifets and Bray [16] by means of the so-called convergent close-coupling (CCC) approach. In this approach, the Lippmann-Schwinger equation for the transition T matrix is solved approximately by introducing a finite set of square-integrable functions to represent both the bound and continuum target states. In this way, the three-body breakup amplitude is actually built up from two-body discrete channel amplitudes. This approach has been recently applied to two-photon DI [17]. The R-matrix formalism which is particularly appropriate for the treatment of one-photon SI has also been used to study the DI problem [18,19]. The most accurate treatment is due to Malegat *et al.* [19] who developed an hyperspherical R-matrix Floquet approach in which semiclassical outgoing waves are used in the asymptotic region to impose three-body boundary conditions. This method has provided accurate results, in particular very close to threshold, for both one-photon SI and DI [20]. An R-matrix Floquet approach using B splines to treat DI of He has also been developed by Feng and van der Hart [21]. Recently, this approach has been generalized to the calculation of the two-photon DI total cross section in He [22]. Finally, McCurdy *et al.* [23] developed a method which, in spirit and formalism, is very close to the Proulx-Shakeshaft approach. This method uses a B-spline implementation of exterior complex scaling.

The study of multiphoton SI and DI processes introduces further difficulties: given the high peak intensity and the ultrashort duration of the XUV pulse, the approaches based on Floquet theory become rapidly numerically untractable. It is therefore necessary to solve nonperturbatively and therefore numerically the corresponding time-dependent Schrödinger equation (TDSE). Needless to say, in contrast to one-photon processes, the high-frequency multiphoton SI and DI processes represent essentially an open problem which has just started to be investigated. There are basically two types of methods to solve numerically the TDSE: The finite difference (FD) grid and spectral methods. Schematically, FD grid methods consist in time propagating the total wave function defined in terms of its finite-difference representation on a spatial grid. Such methods are in fact local in the sense that the spatial derivatives of the total wave function at a given grid point depend on the value of the wave function at neighboring grid points; this leads to the manipulation of rather sparse matrices. In the case of the spectral methods, and for reasons which will be clarified later, the total wave function is first expanded in terms of the eigenstate wave functions of the atomic Hamiltonian, the coefficients being time dependent. These eigenstate wave functions are in turn expanded in a finite basis of trial functions of the electron coordinates. Test functions are then introduced to ensure that the stationary Schrödinger equation is satisfied as closely as possible by the truncated series expansion. This is achieved by minimizing with respect to a suitable norm, the residual—i.e., the error in the stationary Schrödinger equation produced by using the truncated expansion instead of the exact solution. This leads to a generalized eigenvalue problem. The trial functions are usually L^2 integrable functions solutions of a Sturm-Liouville problem. They are chosen according to the physics of the problem and its asymptotic conditions. In general, the test functions are either the same as the trial functions, or Dirac δ functions. In the latter case, we obtain a so-called collocation spectral method which consists in imposing that the solution is correct in all the points of a given grid. These points usually correspond to the abscissae of a Gauss-type quadrature. Let us stress that in contrast to FD methods, the collocation method (and in general all spectral methods) is global because the spatial derivatives of the solution wave function at a given grid point involve all the other grid points. Despite the fact that for a long time—i.e., since the early works of Hartree—FD methods have been considered more accurate than the use of limited basis sets, spectral methods have notable strengths. For analytical functions, errors typically decay at an exponential rather than a (much slower) polynomial rate as a function of the number of trial functions. This approach is surprisingly powerful for many cases with nonsmooth or even discontinuous functions [24]. Especially in several space dimensions, the relatively coarse grids which suffice for most accuracy requirements lead to very time- and memory-effective calculations. Finally, the fact that the solution wave function is expressed in terms of a finite sum of known analytical functions makes the extraction of valuable information (evaluation of observables, momentum-space representation, etc.) more tractable than in the case of FD grid methods.

As in the case of the time-independent methods, the theoretical description of the asymptotic conditions for the complete fragmentation of the target system remains a fundamental problem for both FD grid and spectral methods. In addition to the fact that the two-electron single- and double-continuum states may be degenerate in energy, the numerically built positive-energy states contain necessarily both single- and double-continuum components because they are calculated in a finite space. As a result, it is extremely difficult to disentangle the single- and double-ionization contributions.

A fully numerical integration of the TDSE for laser-driven He has been performed by Taylor and co-workers [25] in a broad range of wavelengths from 780 nm (Ti:sapphire laser) to 14 nm. The approach, which requires considerable computer resources, is based on a mixed-basis set, a FD method in which the radial coordinates r_1 and r_2 of the two electrons are modeled on a FD grid and the four angular coordinates

θ_1, θ_2, ϕ_1, and ϕ_2 are handled by writing the wave function on a basis set of coupled spherical harmonics. The time propagation is carried out by means of an explicit scheme. Colgan *et al.* [26] developed a time-dependent close-coupling theory describing one- and two-photon DI processes in He, Li, and Be. Their method, which is very similar to the method of Taylor and co-workers is also based on a mixed angular basis set and a finite-difference method for the radial part of the total wave function. However, they differ in the way the SI and DI probabilities are calculated. In the approach of Taylor and co-workers, the two-electron radial space is divided into four regions associated with a given ionization stage of He. The size of each of these regions is fixed with some degree of arbitrariness. In the approach of Colgan *et al.*, the DI probability is obtained by projecting the target wave function after the time propagation on an uncorrelated product of Coulomb wave functions. With this method, Colgan *et al.* evaluated one- and two-photon total and differential DI cross sections in He [27,28] with an unexpected accuracy in many cases. This raises the unsolved question of the role of the electronic correlation in the final state. In principle, the final wave function has to be projected on a (multichannel) scattering wave function with the correct asymptotic behavior. Note that the presence of the electron-electron interaction introduces already a phase shift which is essentially built at short distances. Recently, Kleiman *et al.* [29] extended the same approach to one-photon double photoionization with excitation as well as triple ionization of Li.

A spectral method of configuration interaction type to solve the TDSE has been developed by Laulan and Bachau [30,31] for He, H^-, and Be. Products of *B*-spline functions are used to represent the radial part of the atomic states while the angular part is expressed in terms of coupled spherical harmonics. *B*-spline functions offer the advantage of solving the problem in a box, making the control of the density of continuum states easier [32]. In the case of two-photon DI of He, Laulan and Bachau [33] studied the role of the electronic correlation in the final state by projecting the final wave function (after propagation) on a double-continuum state in which the electron-electron repulsion term is treated within zero- and first-order perturbation theory. Their results show no significant effect of the final-state electron correlation for the total DI probability. There is, however, a clear influence of this final-state electron correlation on the electron energy distribution. As a matter of fact, the maximum of the electron energy distribution is closer to the energy conservation line when the first-order correction is introduced.

In the contribution, we present and discuss a spectral method in which the radial part of the wave function is expanded in terms of products of real or complex Coulomb-Sturmian functions in the coordinates r_1 and r_2 and coupled spherical harmonics for the angular coordinates θ_1, θ_2, ϕ_1, and ϕ_2. This method has been briefly and partially described in various situations [34–37]. We believe, however, that we have now reached a stage where we have significant progress to report. In particular, we show that by combining this approach with the *J*-matrix method developed by Heller and Yamani [38], it is possible to treat correctly the correlation in the final state within a time-dependent scheme.

This contribution is structured as follows. After this long introduction where we tried to give an account of the main theoretical approaches developed so far to treat one- and multiphoton SI and DI processes, we present in Sec. II the basic framework of our theoretical approach. This section is divided into three parts. The first part is devoted to structure calculations. We show that very accurate singly and doubly excited states are generated by solving a generalized eigenvalue problem within our spectral method. In the second part, we give a brief account of the *J*-matrix method and generate a multichannel continuum wave function of a two-electron system. The accuracy of this method is then tested by calculating the photoionization (with or without excitation of the residual ion) cross section in various situations. The last part of this section is devoted to the time propagation and to the calculation of the relevant observables. In Sec. III, we test our approach in the case of one-photon SI as well as one-photon DI of He and H^- where accurate data exist. Then, we calculate and analyze the total cross section of two-photon direct DI of He. Unless stated, atomic units are used throughout this work.

II. THEORETICAL APPROACH

A. Atomic structure calculations

1. Spectral expansion of the atomic states

The bound-state wave function of a two-electron system with total angular momentum L of projection M and total energy E_α satisfies the time-independent Schrödinger equation

$$(H - E_\alpha)\Psi_\alpha^{L,M}(\vec{x}) = 0, \tag{1}$$

where $\vec{x}$ stands for all electron position vectors. The non relativistic Hamiltonian H reads

$$H = -\frac{1}{2}\nabla_{r_1}^2 - \frac{1}{2}\nabla_{r_2}^2 - \frac{Z}{r_1} - \frac{Z}{r_2} + \frac{1}{r_{12}}. \tag{2}$$

Z denotes the charge of the nucleus, which is assumed to be infinitely massive. r_1 and r_2 are the radial coordinates of electrons 1 and 2, respectively. $r_{12}=|\vec{r}_1-\vec{r}_2|$ is the interelectronic distance. We now introduce our spectral method aimed at solving Eq. (1). All spectral methods are actually based on the expansion of the solution $\Psi_\alpha^{L,M}$ in a truncated series of the form

$$\Psi_{\alpha,N}^{L,M}(\vec{x}) = \sum_{\nu=1}^{N} \psi_{\alpha,\nu}^{L,M}\Phi_\nu(\vec{x}). \tag{3}$$

ν is associated with a given set of basis parameters. N gives the number of trial (or basis) functions $\Phi_\nu(\vec{x})$. The N expansion coefficients $\psi_{\alpha,\nu}^{L,M}$ are calculated by annuling the residual R_N [39],

$$R_N(\vec{x}) = (H - E_\alpha)\Psi_{\alpha,N}^{L,M}(\vec{x}), \tag{4}$$

in an approximate sense by setting to zero the scalar product

$$\langle R_N, \varphi_\nu \rangle = \int R_N \varphi_\nu w d\vec{x}, \quad \beta = 1, \ldots, N. \tag{5}$$

The φ_ν are the test (or weighting) functions, and the weight w is associated with the type of spectral method and with the trial functions. If the test functions coincide with the trial functions, we obtain the so-called Galerkin spectral method in which the residual R_N is equal to 0 in the mean. When the test functions are given by a product $\Pi_i \delta(\vec{x}_i - \vec{x})$ and the weight w equal to 1, we obtain a collocation method in which the residual R_N is forced to be zero at the collocation points $(\vec{x}_i)$. Such a method is similar to a FD grid method except that the choice of the collocation points is not arbitrary but related to the choice of trial functions. In most of cases, the N collocation points are the abscissae of a Gauss quadrature method; very often, this leads to a faster (exponential) convergence in terms of the number of points [24].

In the present case, we use a Galerkin spectral method. At this stage, two types of basis can be considered: the so-called explicitly correlated (EC) bases in which the basis functions depend explicitly on the interelectronic distance r_{12} and the configuration interaction (CI) bases in which the wave function is written as a linear combination of (antisymmetrized) products of one-electron wave functions. EC bases involve either Hylleraas functions [40] of the form $r_1^k r_2^m r_{12}^n e^{-\alpha r_1} e^{\beta r_2}$ with k, m, and n non-negative integers and α and β positive nonlinear parameters, or functions of the perimetric coordinates [41] $u = -r_1 + r_2 + r_{12}$, $v = r_1 - r_2 + r_{12}$, and $w = r_1 + r_2 - r_{12}$. These EC bases lead to a very accurate description of the energy and wave function of the ground state as well as singly or doubly excited states characterized by a small interelectronic distance. Note that in the case of an EC basis expansion in terms of Coulomb-Sturmian functions (see [42,43] and below) of the perimetric coordinates, the matrix associated with the Hamiltonian (2) is banded and all its elements are calculated analytically [44]. This allows a treatment of matrices of considerable size and accurate calculation of the energy of many singly or doubly excited states. However, the matrix size needed in the case of very asymmetrically excited states (characterized by a relatively large interelectronic distance) becomes rapidly prohibitive and is essentially limited to small total angular momenta $L = 0, 1$.

In the case of the CI bases, one exploits the multipole expansion of the electron-electron Coulomb repulsion:

$$\frac{1}{r_{12}} = \sum_{q=0}^{\infty} \sum_{p=-q}^{q} \frac{4\pi}{2q+1} \frac{r_<^q}{r_>^{q+1}} Y_{q,p}^*(\hat{r}_1) Y_{q,p}(\hat{r}_2), \tag{6}$$

where $r_< = \min(r_1, r_2)$ and $r_> = \max(r_1, r_2)$. The angular part of the wave function in a CI scheme is expressed in terms of bipolar harmonics [45] that couple the individual angular momenta ℓ_1 and ℓ_2 of electrons 1 and 2, respectively, to the resulting total angular momentum L. Hence, electronic correlation is taken into account in CI calculations by including various (ℓ_1, ℓ_2) pairs that are mixed in the infinite sum in Eq. (6). The accuracy of the CI results depends on the number of radial functions in the basis set, as well as the number of angular configurations included.

Due to their simplicity and flexibility, CI bases have been widely used in many-electron atomic and molecular calculations using, for instance, Slater-type functions [46], B splines [32], or hydrogenlike wave functions [47]. Indeed, the CI approach has many interesting features. Its implementation involves the evaluation of one- and two-dimensional integrals, in contrast to EC bases where three-dimensional integrals have to be evaluated. This feature makes the extension of the CI approach to larger systems (with three or more electrons) easy and straightforward contrary to the EC basis expansion approach. Unfortunately, the CI approach has always been plagued with the difficulty of slow convergence in terms of the number of radial functions and angular configurations used. This slow convergence, which is particularly acute for the ground-state energy, is essentially due to the fact that the CI expansions do not satisfy the Kato cusp condition associated with the coalescence of the two electrons [48]. Indeed, the wave function of the system has a discontinuous derivative when $r_1 = r_2$. For a high asymmetrically excited state (HAES), however, in which one electron is in a highly excited level while the other remains in a lower one, there is little overlap between the two electron clouds. In that case, the CI expansion is expected to converge more rapidly and give accurate results. Despite the fact that EC basis expansions are usually preferred because of their accuracy and fast convergence, we use here a CI expansion for two reasons: first, we show that by adequately constructing the CI expansion, it may be the best *ab initio* approach to treat HAES's; second, this type of approach is the most tractable one by far, when dealing with the calculation of the observables in the present context of the time-dependent treatment of multiphoton ionization of two-electron systems by short-wavelength radiation.

Providing an accurate description of HAES's in two-electron systems has been a long-standing problem in theoretical atomic physics. Variational calculations yield very accurate energies for low-lying states in He, but for (singly) excited states having increasingly large principal quantum number n, the accuracy and convergence of the results with increasing basis size deteriorate rapidly. Improvements in CI expansions have made possible the extension of variational calculations in He for $L = 0$ to the intermediate-n range (n up to 18) [49]. However, the deterioration of the accuracy with increasing degree of excitation of one of the electrons prevails (see, e.g., [50]) and has prevented direct application of variational calculations to higher Rydberg states. For higher L-bound states, asymptotic expansions based on a core polarization model have been considered as the only reliable approach due to difficulties encountered by various *ab initio* variational calculations based on explicitly correlated expansions (see, e.g., [51,52].). The difficulty in describing HAES's is due to the fact that two distinct regions of space are associated with the electron probability distribution: a region close to the nucleus for the inner electron and a region far from the nucleus for the highly excited outer electron. A basis expansion will be efficient in describing such a state if it adequately spans these two regions. In this contribution, we construct such basis expansion for a two-electron wave function by combining the structure of the CI expansion and the properties of the Coulomb-Sturmian functions. Before

describing this method, it is worth mentioning that a substantial improvement in the speed of convergence and the accuracy of the CI method has been achieved by Goldman [53] through the so-called modified configuration interaction (MCI) method. In this method, the one-electron functions depend on $r_<$ and $r_>$, which allows for a better representation of the cusp. Furthermore, the angular convergence is improved by increasing the number of angular configurations mixed through the introduction of an *a priori* superposition of angular functions that depend on a set of nonlinear parameters. Unfortunately, the extreme simplicity of the radial integrals in the standard CI method is lost and it seems more difficult to extend the MCI to three- or more-electron systems than the standard CI. In addition, the optimization procedure of the nonlinear parameters requires many steps with each time, the diagonalization of the Hamiltonian matrix. When the matrix is large, such optimization is very time consuming.

The solution of Eq. (1) is expanded as follows (from now on, we drop the suffix N for clarity):

$$\Psi_\alpha^{L,M}(\vec{r}_1,\vec{r}_2) = \sum_{\ell_1,\ell_2} \sum_s \sum_{n_1,n_2} \psi_{k_{1s}k_{2s}n_1n_2\alpha}^{\ell_1\ell_2LM} \times \mathcal{A}\frac{S_{n_1\ell_1}^{k_{1s}}(r_1)}{r_1}\frac{S_{n_2\ell_2}^{k_{2s}}(r_2)}{r_2}\Lambda_{\ell_1\ell_2}^{LM}(\hat{r}_1,\hat{r}_2), \quad (7)$$

where $\psi_{k_{1s}k_{2s}n_1n_2\alpha}^{\ell_1\ell_2LM}$ is the expansion coefficient. The operator $\mathcal{A}$ projects onto either singlet or triplet states, so as to ensure the symmetry or antisymmetry of the spatial wave function as required by the Pauli principle. This operator is defined by $(1+\epsilon P)/\sqrt{2}$ where the operator P exchanges both electrons and ϵ takes the value $+1$ for singlet states and -1 for triplet states. The radial one-electron functions $S_{n,\ell}^k(r)$ are Coulomb-Sturmian functions [42,43] defined for a given angular momentum ℓ and radial index n by

$$S_{n,\ell}^k(r) = N_{n,\ell}^k r^{\ell+1} e^{-kr} L_{n-\ell-1}^{2\ell+1}(2kr), \quad (8)$$

where k is a nonlinear parameter assumed real for the time being. $L_{n-\ell-1}^{2\ell+1}(2kr)$ is a Laguerre polynomial. The normalization constant $N_{n,\ell}^k$ given by

$$N_{n,\ell}^k = \sqrt{\frac{k}{n}}(2k)^{\ell+1}\left(\frac{(n-\ell-1)!}{(n+\ell)!}\right)^{1/2} \quad (9)$$

is derived from the condition $\int_0^\infty S_{n,\ell}^k(r)S_{n,\ell}^k(r)dr=1$. The radial index n of the Sturmian functions is a positive integer satisfying $n \geqslant \ell+1$. The angular part of the expansion (7) is expressed in term of bipolar spherical harmonics [45],

$$\Lambda_{\ell_1,\ell_2}^{LM}(\hat{r}_1,\hat{r}_2) = \sum_{m_1,m_2} \langle \ell_1 m_1 \ell_2 m_2 | LM\rangle Y_{\ell_1,m_1}(\hat{r}_1) Y_{\ell_2,m_2}(\hat{r}_2), \quad (10)$$

which couple the two individual angular momenta ℓ_1 and ℓ_2 in the L-S scheme. $Y_{\ell,m}$ denotes the spherical harmonic, and $\langle \ell_1 m_1 \ell_2 m_2 | LM\rangle$ is the Clebsch-Gordan coefficient. In order to preserve parity, which is a good quantum number, the L-S coupled individual angular momenta of the electrons must satisfy $(-1)^L=(-1)^{\ell_1+\ell_2}$ [54]. In order to avoid redundances in expansion (7), the orbital angular momenta are restricted to $\ell_1 \leqslant \ell_2$, and if $\ell_1=\ell_2$, then $n_1 \leqslant n_2$.

The Coulomb-Sturmian functions (8) are a solution of the Sturm-Liouville problem

$$\left[-\frac{1}{2}\frac{d^2}{dr^2} + \frac{\ell(\ell+1)}{2r^2} - \frac{\chi}{r} + \frac{k^2}{2}\right] S_{n,\ell}^k(r) = 0, \quad (11)$$

with the associated boundary conditions $S_{n,\ell}^k(0)=0$ and $S_{n,\ell}^k(\infty)=0$. χ, equal to kn, is the eigenvalue, and k is fixed and real. Coulomb-Sturmian functions have interesting features that are very suitable for a reliable CI method. (i) They form a complete and discrete basis set of L^2 integrable functions. (ii) They are exact solutions of the stationary Schrödinger equation for a single electron in the Coulomb field of a nucleus of charge Z; when $k=Z/n$, the Coulomb-Sturmian function $S_{n,\ell}^k(r)$ coincides with the hydrogenic bound state of principal quantum number n and angular momentum quantum number ℓ. (iii) Their associated nonlinear parameter k and index n both act like spatial dilatation factors. Indeed, for n and ℓ fixed, decreasing (increasing) k increases (decreases) the radial spread of $S_{n,\ell}^k$. Similarly, increasing (decreasing) n with k and ℓ fixed increases (decreases) the radial spread of $S_{n,\ell}^k(r)$. Therefore, nonlinear parameters and radial indices of Sturmian functions could be adjusted in the basis expansion in order to adequately span the two distinct regions mentioned earlier in HAES's. This requires the basis expansion to be built in such a way that the nonlinear parameter and the number of Sturmian functions attributed to one electron could be different from those attributed to the other.

Note that in all previous CI expansions involving Coulomb-Sturmian functions the same nonlinear parameter k is used for all Coulomb-Sturmian functions in the basis. This corresponds to setting $k_{1s}=k_{2s}\equiv k$ and $s=1$ in our expansion (7). Futhermore, for each pair (ℓ_1,ℓ_2), the same number N of Coulomb-Sturmian functions $S_{n_1,\ell_1}^k(r_1)$ with $\ell_1+1 \leqslant n_1 \leqslant \ell_1+N$ and $S_{n_2,\ell_2}^k(r_2)$ with $\ell_2+1 \leqslant n_2 \leqslant \ell_2+N$ is taken into account. On the one hand, solving the stationary Schrödinger equation with such a basis is quite simple because all integrals involving the Coulomb-Sturmian functions can be obtained by means of simple analytical formulas and because both the overlap and the independent electron Hamiltonian (given by $h=H-1/r_{12}$) have a banded structure. On the other hand, considering the dilatation properties mentioned above for the nonlinear parameter and the Sturmian index, using identical parameters for the two electrons means that they are treated as if their clouds were localized at similar distances from the nucleus. Intuitively, this means that this approach must be adequate only for describing the ground state or symmetrically excited states where the individual quantum states of the two electrons are almost identical. But for HAES's, where the two electron clouds are located in quite different regions, the approach would be inadequate because the basis functions fail to properly span the two regions. Therefore, such a CI approach turns out to be globally limited. In the case of the ground state, it is the cusp problem that limits the accuracy of the CI expansion unless a large number of pairs (ℓ_1,ℓ_2) is taken into account. In the case of

the HAES's, it is the use of a single k and N that limits the accuracy. Note that within such a scheme a good description of the HAES's would require N to be very large for both electrons although a small number of Coulomb-Sturmian functions is sufficient to describe the inner electron.

We propose a Coulomb-Sturmian basis expansion (7) that overcomes the limitations mentioned above. It is constructed in order to allow the nonlinear parameter and number of Sturmian functions attributed to one electron to be different from those attributed to the other electron. For an accurate description of a HAES with such a basis, according to the dilatation properties of Coulomb-Sturmian functions discussed earlier, a smaller number of Sturmian functions with a relatively large nonlinear parameter would be enough for the inner electron, whereas a larger number of Sturmian functions with a smaller nonlinear parameter would be necessary to describe the outer electron. It follows that only basis functions which are really essential and adequate for the description of a given atomic state or any physical process may be introduced in the basis, leading to a substantial reduction of the basis size. In practice, we introduce a set of Coulomb-Sturmians functions (SCSF)—i.e., a combination $[k_{1s},N_{1s},k_{2s},N_{2s}]$ involving the Coulomb-Sturmian functions $S^{k_{1s}}_{n_1,\ell_1}(r_1)$ with $\ell_1+1 \leqslant n_1 \leqslant \ell_1+N_{1s}$ associated with electron 1 and $S^{k_{2s}}_{n_2,\ell_2}(r_2)$ with $\ell_2+1 \leqslant n_2 \leqslant \ell_2+N_{2s}$ associated with electron 2. The pairs (k_{1s},N_{1s}) and (k_{2s},N_{2s}) are to be adjusted for each electron in order to increase the density of Coulomb-Sturmian functions in the two characteristic regions of the HAES's. Good nonlinear parameters for describing a given atomic state are consistently obtained by exploiting the fact that $S^k_{n,\ell}(r)$ describes an electron of energy $\varepsilon=-k^2/2=-Z^2/2n^2$ in the field of a nucleus of charge Z. Consider, for instance, a bound state of He with electron 1 in the $1s$ state and electron 2 in an excited state with principal quantum number n_2. These electrons experience effective charges 2 and $Z-\sigma$, respectively, where $\sigma(0<\sigma\leqslant 1)$ results from screening by the inner electron. Such a state is accurately described by including in the basis expansion, a SCSF characterized by nonlinear parameters $k_1=2$ and $k_2=(Z-\sigma)/n_2$. For each pair (ℓ_1,ℓ_2), one or many SCSF [labeled in Eq. (7) by the index s] may be selected. The use of many SCSF's allows us to span a larger region with the basis and consequently permits a simultaneous description of many eigenstates with a single wave function expansion. As the degree of excitation of the outer electron increases, only N_{1s} or N_{2s} (not both) has to be increased and the corresponding nonlinear parameter decreased in the basis. On the other hand, as this degree of excitation increases, the correlation between the two electrons decreases and therefore less angular configurations are necessary in the basis for accurate results, so that the overall basis size is kept within reasonable limits.

So far, we have assumed that the nonlinear parameters are real. However, by making these parameters complex, our spectral expansion (7) may be used to describe accurately the doubly excited states. We write

$$k \to ke^{-i\theta}, \tag{12}$$

where $0<\theta<\pi/2$. Mathematically, expanding the solution of Eq. (1) in terms of complex Coulomb-Sturmian functions amounts to transforming the atomic Hamiltonian (2) by a complex scaling $r_i \to r_i \exp(i\theta)$ and expanding the eigenfunctions of the scaled Hamiltonian on the real Coulomb-Sturmian functions. In this picture, varying the angle θ from 0 to $\pi/2$, while leaving the bound states unaffected, rotates the continuum spectrum into the lower half plane by an angle 2θ about each threshold, thereby uncovering the resonances and making them amenable on a L^2 basis. From the physical point of view, expanding the solution of Eq. (1) in terms of complex Coulomb-Sturmian functions reinforces the boundary conditions associated with the ionization problem (which is our ultimate goal): namely, an outgoing spherical wave. Note that a basis of complex Coulomb-Sturmian functions characterized by only one complex nonlinear parameter is not complete anymore. Furthermore, with our convention for the angle θ [see Eq. (12)], an outgoing spherical wave can be expanded on this basis, with decreasing coefficients for increasing values of the Sturmian radial index while the expansion of ingoing spherical waves diverges [55].

Finally, another interest in using Coulomb-Sturmian functions is that obtaining the two-electron wave function in momentum space is straightforward. This feature is particularly important in the perspective of a time-dependent study of two-electron systems in the presence of ultrashort, electromagnetic pulses. Indeed, by taking the Fourier transform of Eq. (7), one obtains a similar expression for the wave function in momentum space, but with the radial Coulomb-Sturmian functions $S^k_{n,\ell}(r)$ replaced by their counterpart $\Sigma^k_{n,\ell}(p)$ in momentum space, which is given by

$$\Sigma^k_{n,\ell}(p) = \mathcal{N}^k_{n,\ell} \frac{p^\ell}{(p^2+k^2)^{\ell+2}} C^{\ell+1}_{n-\ell-1}\left(\frac{p^2-k^2}{p^2+k^2}\right), \tag{13}$$

where $C^{\ell+1}_{n-\ell-1}$ denotes the Gegenbauer polynomial [56]. The condition $\int_0^\infty \Sigma^k_{n,\ell}(p)\Sigma^k_{n,\ell}(p)p^2dp=1$ is used to derive the normalization constant

$$\mathcal{N}^k_{n,\ell} = 2^{2\ell+2}k^{\ell+2}\ell! \sqrt{\frac{2kn}{\pi}\frac{(n-\ell-1)!}{(n+\ell)!}}. \tag{14}$$

2. Solution of the stationary Schrödinger equation

After substituting $\Psi^{L,M}_\alpha$ in Eq. (4) by its expansion (7) and setting to zero the scalar products (5), we obtain the following generalized eigenvalue problem:

$$\mathbf{H\Psi} = E\mathbf{S\Psi}, \tag{15}$$

where $\mathbf{\Psi}$ is the vector representation of the wave function Ψ. $\mathbf{S}$ is a real symmetric matrix representing the overlap while $\mathbf{H}$ is the matrix associated with the atomic Hamiltonian. $\mathbf{H}$ is either real symmetric for real nonlinear parameters or complex symmetric for complex nonlinear parameters. The calculation of the matrix elements of $\mathbf{S}$ and $\mathbf{H}$ may be performed analytically; it becomes, however, very cumbersome as soon as various sets of nonlinear parameters are introduced. Instead, we use a Gauss-Laguerre quadrature which is particularly appropriate and, in principle, exact in the present case since all the integrals to calculate involve products of polynomials and decreasing exponentials. Care, however,

must be taken in calculating the elements of the matrix associated with the $1/r_{12}$ term. These elements involve the following double radial integral [see Eq. (6)]:

$$U = \int_0^\infty dr_1 \int_0^\infty dr_2 S^{k_1'}_{n_1',\ell_1'}(r_1) S^{k_2'}_{n_2',\ell_2'}(r_2) \left(\frac{r_<^q}{r_>^{q+1}} \right) \times S^{k_1}_{n_1,\ell_1}(r_1) S^{k_2}_{n_2,\ell_2}(r_2). \quad (16)$$

In order to apply a Gauss-Laguerre quadrature while avoiding severe round-off errors, it is necessary to rewrite this double integral as follows:

$$U = \int_0^\infty dr_2 S^{k_2'}_{n_2',\ell_2'}(r_2) S^{k_2}_{n_2,\ell_2}(r_2) r_2^q \int_{r_2}^\infty dr_1 S^{k_1'}_{n_1',\ell_1'}(r_1) \times S^{k_1}_{n_1,\ell_1}(r_1) \frac{1}{r_1^{q+1}} + \int_0^\infty dr_1 S^{k_1'}_{n_1',\ell_1'}(r_1) S^{k_1}_{n_1,\ell_1}(r_1) r_1^q \int_{r_1}^\infty dr_2 S^{k_2'}_{n_2',\ell_2'}(r_2) \times S^{k_2}_{n_2,\ell_2}(r_2) \frac{1}{r_2^{q+1}}. \quad (17)$$

The above decomposition is not the conventional one which consists in writing

$$U = \int_0^\infty dr_1 S^{k_1'}_{n_1',\ell_1'}(r_1) S^{k_1}_{n_1,\ell_1}(r_1) \frac{1}{r_1^{q+1}} \int_0^{r_1} dr_2 S^{k_2'}_{n_2',\ell_2'}(r_2) \times S^{k_2}_{n_2,\ell_2}(r_2) r_2^q + \int_0^\infty dr_1 S^{k_1'}_{n_1',\ell_1'}(r_1) S^{k_1}_{n_1,\ell_1}(r_1) r_1^q \int_{r_1}^\infty dr_2 S^{k_2'}_{n_2',\ell_2'}(r_2) \times S^{k_2}_{n_2,\ell_2}(r_2) \frac{1}{r_2^{q+1}}. \quad (18)$$

In order to use a Gauss-Laguerre quadrature, it is still necessary in this latter case to rewrite the first inner integration over r_2 as a difference between an integration from 0 to ∞ and an integration from r_1 to ∞ so that U is now written as a sum of three terms. It turns out that very often, two of these three terms cancel out almost exactly, therefore introducing serious round-off errors. Instead, the decomposition (17) revealed very stable numerically. We have checked that even for large values of the radial index ($\simeq$140) and of the angular quantum numbers (around 15) the calculation of the integrals (17) is free of round-off errors. For a given total angular momentum L, the matrix $\mathbf{H}$ is completely full because of the $1/r_{12}$ term while $\mathbf{S}$ has a block-diagonal structure, each diagonal block corresponding to a given pair (ℓ_1, ℓ_2). For each diagonal block, there may be one or many subblocks, each one associated with a SCSF selected for the pair (ℓ_1, ℓ_2) in question. Note that because different SCSF's may be used, the size of matrices $\mathbf{S}$ and $\mathbf{H}$ may vary with L.

The inclusion of many sets of real nonlinear parameters in our basis makes it numerically "overcomplete." It means that some eigenvalues of the overlap matrix (which must be positive definite) can be zero or even negative. This results from the loss of numerical linear independence due to the finite precision with which numbers are stored. Therefore, the inversion of this overlap matrix gives rise to serious numerical overflows. In order to solve this problem, we can proceed as follows. Let $\mathbf{H}$ and $\mathbf{S}$ be $(n \times n)$ matrices, and let us consider the $(n \times n)$ orthogonal matrix $\mathbf{T}$ that diagonalizes $\mathbf{S}$. Therefore, $\mathbf{T}^t\mathbf{S}\mathbf{T} = \mathbf{s}$ where $\mathbf{s}$ is the diagonal matrix containing the eigenvalues of $\mathbf{S}$ whose associated eigenvectors are stored in columns of $\mathbf{T}$. We define a small and positive cutoff ϵ (of the order of 10^{-12}) and reject all eigenvalues of $\mathbf{S}$ that are smaller than this cutoff. We denote by p the number of overlap eigenvalues that are greater or equal to the cutoff. After rejecting the $n-p$ overlap eigenvalues and their corresponding eigenvectors, the sizes of $\mathbf{T}$ and $\mathbf{s}$ are, respectively, reduced to $(n \times p)$ and $(p \times 1)$. Using basic matrix algebra, one can show that Eq. (15) can be transformed into the simple eigenvalue problem

$$\tilde{\mathbf{H}}\tilde{\mathbf{\Psi}} = E\tilde{\mathbf{\Psi}}, \quad (19)$$

with

$$\tilde{\mathbf{H}} = \mathbf{V}^t\mathbf{H}\mathbf{V}, \quad (20)$$

$$\tilde{\mathbf{\Psi}} = \mathbf{V}^{-1}\mathbf{\Psi}. \quad (21)$$

$\tilde{\mathbf{H}}$ is a $(p \times p)$ matrix and $\tilde{\Psi}$ is a $(p \times 1)$ vector. $\mathbf{V}$ is a $(n \times p)$ matrix given by

$$\mathbf{V} = \mathbf{T}\mathbf{s}^{-1/2}. \quad (22)$$

The resulting simple eigenvalue problem (19) can be solved by using standard diagonalization techniques. The above procedure, however, has a drawback: the number of eigenvalues that are eliminated can be very large (up to 10% of the total number of eigenvalues in some cases). Whether or not the corresponding eigenvectors that are eliminated play a role is not clear. Therefore, instead of eliminating eigenvalues of the overlap matrix and in order to keep this matrix positive definite, we add to the overlap matrix $\mathbf{S}$ a diagonal matrix $\mathbf{R}$ whose diagonal elements are tiny random numbers (of the order of 10^{-13} corresponding to the double-precision machine accuracy). We then diagonalize the modified overlap matrix $\mathbf{S}' \equiv \mathbf{S} + \mathbf{R}$ and use its eigenvectors to regenerate our basis. These eigenvectors are orthonormal and barely differ from those of $\mathbf{S}$. By using the Wielandt-Hoffman theorem [57], it has been shown [58] that if $\max(R_{ii})$ is of the order of 10^{-13}, we have

$$|v'^t\mathbf{S}v' - v^t\mathbf{S}v| \approx 10^{-13}\sqrt{n}, \quad (23)$$

where v' and v are normalized eigenvectors of $\mathbf{S}'$ and $\mathbf{S}$, respectively. n is the dimension of these vectors. This shows clearly that the difference between v' and v is indeed very small.

3. Bound and resonant states of He and H^-

In this section, we consider He and H^- and analyze the accuracy obtained within our approach for the ground-state as well as the singly and doubly excited-state energies. Table

TABLE I. Convergence of the ground-state energy in a.u. of He and H^- as a function of the number of pairs of electron angular momenta. The size refers to the number of terms in the expansion of the wave function. Reference data in bold characters are from [51].

(ℓ_1,ℓ_2)	Size	He $-E$	H^- $-E$
(0,0)	465	2.87902797	0.51449614
(1,1)	930	2.90051386	0.52658410
(2,2)	1395	2.90276209	0.52743744
(3,3)	1860	2.90331321	0.52762391
(4,4)	2325	2.90350682	0.52768618
(5,5)	2790	2.90358925	0.52771215
(6,6)	3255	2.90362816	
(7,7)	6560	2.90366100	
		2.9037243770	**0.5277510165**

I illustrates the convergence with respect to (ℓ_1,ℓ_2) of the ground-state energy for He and H^-. Our reference data are from [59]. In this case, we use only one set of Coulomb-Sturmian functions (k_1,N_1,k_2,N_2): (2.0,40,2.0,40) for He and (1.0,40,1.0,40) for H^-. Note that, with the inclusion of more pairs (ℓ_1,ℓ_2), the number of Sturmian functions (N_1 and N_2) per electron should increase since higher values of the angular momenta contribute to the large-distance behavior of the wave function. Nevertheless, even for these fixed and rather high values of N_1 and N_2, the convergence is expected to be slow because, as mentioned before, our CI approach does not fulfill the Kato cusp condition associated with the two-electron coalescence. It is worth noticing, however, that the accuracy we achieve, 5 digits with 9 pairs of angular momenta, is more than enough for the time propagation which is our ultimate goal. In addition, our results compare very well with those of Venuti and Decleva [60] for H^-, who used a CI type of approach based on *B*-spline functions. They obtain 7 digits accuracy with 50 *B* splines per electron and 25 pairs of angular momenta.

The convergence as well as the accuracy of the results increases significantly as the asymmetry of the states increases. This is clearly demonstrated in Table II where we consider the $4\,^3F$ and $8\,^3K$ states of He and compare with the extremely accurate reference data of Drake [51]. With an expansion of only 144 terms and 7 pairs of angular momenta, we obtain energies within a relative uncertainty of about 10^{-8} for the $4\,^3F$ state and 10^{-13} for the $8\,^3K$ state. As in the previous case, the energy of these states has been obtained by selecting only one set of Coulomb-Sturmian functions (2.0,2,0.4,12) for the $4\,^3F$ state and (2.0,2,0.17,12) for the $8\,^3K$ state. It is important to stress that the values of the nonlinear parameters are now different. In the case of the $4\,^3F$ state, for instance, we set $k_1=2.0$ to describe the inner electron and $k_2=0.4$ for the outer electron. A similar convergence has been obtained for the corresponding singlet states $4\,^1F$ and $8\,^1K$ (see [36]).

One of the objectives of the present approach is to generate accurately many singly and doubly excited states from a single diagonalization while keeping the size of the basis within reasonable limits. This is achieved by introducing, for any given total angular momentum *L*, various sets of Coulomb-Sturmian functions. For the sake of illustration, we show in Tables III and IV the 50 lowest singly excited singlet states in He for $L=7$. Seven pairs (ℓ_1,ℓ_2) of angular momenta have been considered, and four sets of Coulomb-Sturmian functions per pair have been selected: (2,10,0.2,50), (2,10,0.09,50), (2,10,0.04,60), and (2,10,0.02,60). Results in the literature are very scarce. Drake [51] has obtained extremely accurate data for $n=8$, 9, and 10 by means of a Hylleraas-type variational calculation. As shown in Table III, the agreement between his results and our data is perfect (all digits coincide). Above $n=10$, the accuracy of our data has been checked by analyzing their stability as a function of N_1 and N_2. More than 10 digits are correct in all data presented in Table IV. Provided that N_2 is sufficiently large (due to the number of nodes required to describe correctly the wave function of the outer electron), our method is able to reproduce accurately the energy of high-lying singly excited states.

TABLE II. Convergence of the $4\,^3F$ and $8\,^3K$ state energy in a.u. of He as a function of the number of pairs of electron angular momenta. The size refers to the number of terms in the expansion of the wave function. Reference data in bold characters are from [51].

$4\,^3F$			$8\,^3K$		
(ℓ_1,ℓ_2)	Size	$-E$	(ℓ_1,ℓ_2)	Size	$-E$
(0,3)	24	2.031250032	(0,7)	24	2.00781249999999
(1,2)	48	2.031252292	(1,6)	48	2.00781250587708
(1,4)	72	2.031255100	(1,8)	72	2.00781251256536
(2,3)	96	2.031255117	(2,5)	96	2.00781251256693
(2,5)	120	2.031255143	(2,7)	120	2.00781251256816
(3,4)	144	2.031255144	(2,9)	144	2.00781251257019
(3,6)	168	2.031255145	(3,4)	168	2.00781251257019
−2.03125516840324			**−2.00781251257023**		

TABLE III. Energies in a.u. for the three lowest singly excited singlet states in He for $L=7$. Reference data in bold characters are from Ref. [51].

n	$-E$	n	$-E$
8	2.00781251257020	8	**2.0078125125702293**
9	2.00617284909629	9	**2.0061728490963298**
10	2.00500000738827	10	**2.0050000073883759**

Let us now show that our method applies also to the doubly excited states. However, the size of the basis and, in particular, the number of pairs of electronic angular momenta included must be increased significantly in order to generate accurate energy widths (that may become very small close to the thresholds). In Table V, we present results for the energy and width of triplet S states belonging to a doubly excited Rydberg series below the $N=2$ threshold. We use the $(N,K)_n$ nomenclature: the index N denotes the principal quantum number of the electron in the remaining He^+ ion once the outer electron is ionized. The index n denotes the principal quantum number of the outer electron while the index k ($k=-N+1,-N+3,\ldots,N-3,N-1$) determines the parabolic quantum number of the Stark-type state in which the inner electron resides. k is therefore related to the angle between the two electron position vectors $\vec{r}_1$ and $\vec{r}_2$. In order to calculate the width of these states, we used a complex Coulomb-Sturmian basis or, equivalently, we performed a complex scaling of the atomic Hamiltonian. The angle θ associated to complex scaling is equal to 0.2 rad. Our results are compared with the very accurate data of Bürgers *et al.* [52]. These data have been obtained through a single diagonalization of the atomic Hamiltonian, calculated in an explicitly correlated basis. For small n, where the Kato cusp related to the two-electron coalescence limits convergence for CI bases, our results (energies and widths) agree with the reference data within 10^{-7} a.u. As n increases, the agreement improves, and for $n>5$, the accuracy of our results is of the order or better than 10^{-9}. In the case of the corresponding singlet states (see [36]), the accuracy decreases a little bit because the influence of the Kato cusp of the wave function is more important. In Table VI, we give the real and imaginary parts of the energy of various doubly excited singlet S states belonging to two different Rydberg series that converge towards the $N=2$ and $N=4$ threshold, respectively. These two sets of data have been obtained through a single diagonalization, the basis size being more than 2 times smaller than the size of the explicitly correlated basis used to generate the reference data [52]. We see that the uncertainty in both the real and imaginary parts of the energy is about 10^{-5} a.u. Finally, let us mention that we also calculate oscillator strengths in both length and velocity gauges for bound-bound transitions. They are in very good agreement with all the data we found in the literature.

B. Continuum wave functions

By solving the generalized eigenvalue problem (15) in a real basis, we obtain eigenenergies corresponding to bound states and to continuum states. These continuum states are not the correct continua associated with the atomic Hamiltonian (2) because our L^2 basis is finite. These states are rather (discrete) pseudostates that represent the continuum in a finite space. When the total energy is below the double-ionization threshold but above the first single-ionization threshold, the pseudostates are associated with a single continuum. Above the double-ionization threshold, however, it is impossible to associate a given pseudostate with a single or/and a double continuum. This is because single and double continua essentially differ by their asymptotic behavior which is not described in our finite basis. This is the problem we have to face if we want to calculate the probability of single or double ionization resulting from the interaction of the atomic system with an external field.

In principle, the exact solution of the Hamiltonian (2) in a given continuum channel is a multichannel scattering wave function. This means that the coupling between the continuum channel in question to all the other continuum channels must be taken into account accurately in the calculation of this wave function. This coupling results from the $1/r_{12}$ interaction. Let us first assume that the total energy of the system is negative and higher than the energy of the first single-ionization potential so that the double-ionization channels are closed. Upon this condition, the scattering wave function associated with the single-ionization channel be-

TABLE IV. Energies in a.u. for the next 47 singly excited singlet states in He for $L=7$.

n	$-E$	n	$-E$
11	2.00413223717662	35	2.00040816347356
12	2.00347222679722	36	2.00038580266060
13	2.00295858355916	37	2.00036523027144
14	2.00255102340278	38	2.00034626055087
15	2.00222222468987	39	2.00032873124877
16	2.00195312705554	40	2.00031250013960
17	2.00173010553539	41	2.00029744212801
18	2.00154321134408	42	2.00028344683247
19	2.00138504280678	43	2.00027041655393
20	2.00125000108211	44	2.00025826456815
21	2.00113378778711	45	2.00024691367864
22	2.00103305867120	46	2.00023629498818
23	2.00094518030416	47	2.00022634684952
24	2.00086805619116	48	2.00021701397005
25	2.00080000056386	49	2.00020824664031
26	2.00073964547280	50	2.00020000007186
27	2.00068587150577	51	2.00019223382341
28	2.00063775550570	52	2.00018491130597
29	2.00059453068501	53	2.00017799934821
30	2.00055555588461	54	2.00017146782063
31	2.00052029166162	55	2.00016528930985
32	2.00048828152192	56	2.00015943882037
33	2.00045913707084	57	2.00015389211468
34	2.00043252617865		

TABLE V. Energies (E) and widths (Γ) in a.u. of the $(N,k)_n=(2,1)_n$ triplet Rydberg series in He.

	Bürgers *et al.* [52]		This work	
n	$-E$	$-\Gamma/2$	$-E$	$-\Gamma/2$
3	0.602577505	0.3325(−5)	0.60257748303	0.3296(−5)
4	0.548840858	0.1547(−5)	0.54884085388	0.1533(−5)
5	0.528413972	0.771(−6)	0.52841397047	0.7639(−6)
6	0.518546375	0.428(−6)	0.51854637470	0.4247(−6)
7	0.513046496	0.260(−6)	0.51304649599	0.2578(−6)
8	0.509672798	0.169(−6)	0.50967279751	0.1675(−6)
9	0.507456056	0.116(−6)	0.50745605604	0.1146(−6)
10	0.505922151	0.82(−7)	0.50592215145	0.8153(−7)
11			0.50481701598	0.5991(−7)
12			0.50399459389	0.4564(−7)
13			0.50336609531	0.3547(−7)
14			0.50287502900	0.2804(−7)
15			0.50248406749	0.2252(−7)
16			0.50216774456	0.1834(−7)
17			0.50190820492	0.1513(−7)
18			0.50169262936	0.1262(−7)
19			0.50151162186	0.1063(−7)
20			0.50135816858	0.9033(−8)
21			0.50122694821	0.7735(−8)
22			0.50111386461	0.6670(−8)
23			0.50101572323	0.5788(−8)
24			0.50093000308	0.5052(−8)
25			0.50085469322	0.4432(−8)

haves asymptotically as a dying exponential in these double-ionization channels and as an outgoing wave function in the single-ionization channels. Such a scattering wave function may be generated accurately with the so-called Jacobi- or J-matrix method, which exploits the fact that the Hamiltonian associated with a pure hydrogenic system can be analytically diagonalized in a Coulomb-Sturmian basis. This approach bears close resemblance to the R-matrix theory [61]. As in this latter case, the configuration space is divided into two regions. In the inner region, the space is spanned by a finite Sturmian basis similar to the one used to solve the time-independent Schrödinger equation. Note that in this case, this basis is characterized by only one nonlinear parameter. In the outer region, it is assumed that the outgoing electron moves in a screened Coulomb potential. Furthermore, in order to reproduce the correct asymptotic behavior of the outgoing electron wave function in each channel, it is necessary, at least implicitly, to complete the L^2 basis used in the inner region. In other words, the outgoing electron wave function is expanded in the basis of all Coulomb-Sturmian functions that are not included in the finite basis of the inner region. Upon these conditions, the multichannel scattering

TABLE VI. Real and imaginary parts of the energies (E) in a.u. of some doubly excited singlet S states belonging to the $(N,k)_n=(2,1)_n$ and $(4,-1)_n$ Rydberg series in He.

			Burgers *et al.* [52]		This work	
N	k	n	$-\mathrm{Re}(E)$	$-\mathrm{Im}(E)$	$-\mathrm{Re}(E)$	$-\mathrm{Im}(E)$
2	1	2	0.777867636	0.002270	0.77787	0.002268
2	1	6	0.517641112	0.000057	0.51764	0.000057
2	1	10	0.505759104	0.000010	0.50576	0.000010
4	−1	4	0.168261328	0.001086	0.16826	0.001081
4	−1	10	0.130160039	0.000060	0.13017	0.000067
4	−1	16	0.1269944	0.000017	0.12699	0.000155

wave function may be written in terms of a close-coupling expansion. For a given channel Γ and a given outgoing electron energy E, we write [62]

$$\Theta_\Gamma(E,\vec{r}_1,\vec{r}_2) = \sum_\alpha b_\alpha^\Gamma(E)\Psi_\alpha^{L,M}(\vec{r}_1,\vec{r}_2) + \sum_{\Gamma'}\sum_{n_2=N_2}^{\infty} f_{n_2}^{\Gamma\Gamma'}(E)\Phi_{n_2}^{\Gamma'}(\vec{r}_1,\vec{r}_2), \quad (24)$$

where the channel $\Gamma=(\tilde{n}_1,\ell_1,\ell_2;L,M)$ designates the target radial and angular quantum numbers as well as the angular momentum of the ejected electron, the total two-electron angular momentum, and its projection. The right-hand side (RHS) of expression (24) contains two terms. The first one is the representation of the scattering wave function in the inner region: namely, its expansion in the eigenstates wave function $\Psi_\alpha^{L,M}(\vec{r}_1,\vec{r}_2)$ obtained by diagonalizing the atomic Hamiltonian in our finite basis. These eigenstate wave functions are given by expression (7), in which only one nonlinear parameter denoted here by k is introduced [62]. The second term of the RHS of expression (24) describes the correct asymptotic behavior of the scattering wave function. It is a double expansion over all included channels and over n_2 the radial index of the Coulomb-Sturmian functions associated with the ejected electron. $\Phi_{n_2}^{\Gamma'}(\vec{r}_1,\vec{r}_2)$ is the two-electron wave function in the outer region; it is written as follows:

$$\Phi_{n_2}^{\Gamma'}(\vec{r}_1,\vec{r}_2) = \mathcal{A}\frac{U_{\tilde{n}_1\ell_1}(r_1)}{r_1}\frac{S_{n_2\ell_2}^k(r_2)}{r_2}\Lambda_{\ell_1\ell_2}^{LM}(\hat{r}_1,\hat{r}_2), \quad (25)$$

where $U_{\tilde{n}_1\ell_1}(r_1)$ is the wave function associated with the target bound states and pseudostates which are obtained by diagonalizing the target Hamiltonian in our finite Coulomb-Sturmian basis of radial index n_1, which runs from 1 to (N_1-1) like in the inner basis. n_2 associated with the ejected electron runs from N_2 to ∞. In the present case, ℓ_1 and ℓ_2 are no longer restricted as in Eq. (7) because the two radial orbitals can no longer be identical. In addition, we assume for the time being that $N_1=N_2$. By demanding that $\Theta_\Gamma(E,\vec{r}_1,\vec{r}_2)$ solve the Schrödinger equation for the Hamiltonian in Eq. (2), one obtains an algebraic system of equations to solve for the coefficients $b_\alpha^\Gamma(E)$ and $f_{n_2}^{\Gamma\Gamma'}(E)$. The outer region expansion coefficients are written as follows [62]:

$$f_{n_2}^{\Gamma\Gamma'}(E) = \psi_{n_2}^{\ell_2'}(E-\epsilon_{\tilde{n}_1'}^{\ell_1'})\delta_{\Gamma\Gamma'} - \chi_{n_2}^{\ell_2'}(E-\epsilon_{\tilde{n}_1'}^{\ell_1'})T_{\Gamma\Gamma'}, \quad (26)$$

where $\tilde{n}_1'$, ℓ_1', and ℓ_2' refer to the channel Γ'. $\epsilon_{\tilde{n}_1'}^{\ell_1'}$ is the energy of the target electron. $\psi_{n_2}^{\ell_2'}$ is the expansion coefficient of a regular Coulomb wave in Coulomb-Sturmian functions, while $\chi_{n_2}^{\ell_2'}$ is the expansion coefficient of either an outgoing Coulomb wave for open channels or a dying exponential for closed channels. When $E<\epsilon_{\tilde{n}_1'}^{\ell_1'}$, the channel Γ' is closed, and only the second term contributes, because channel Γ is assumed open. The open part of T is then the transition matrix (to a constant), while the closed part contains the closed-channel coefficients. When the total energy E of the system is negative and therefore lower than the double-ionization potential, all channels associated with the ejection of the target electron ($\epsilon_{\tilde{n}_1'}^{\ell_1'}>0$) are closed. They do, however, contribute to the transition matrix and must be included for the convergence of the calculation. When E becomes positive, these channels open progressively and contribute significantly to the transition matrix. Here, it is important to stress that the double-continuum channels are described in an approximate way. Asymptotically, one of the electrons is described by a Coulomb wave while the other one (the inner one) is described by a pseudostate. It is precisely this type of approximation the CCC approach is based on [17].

The reliability of the present method to generate accurate double-ionization probabilities and cross sections rests on precise knowledge of the multichannel continuum wave functions. It is therefore important to assess the accuracy of the J-matrix method in this context. In the following we consider the photodetachment of H^- for photon energies both below and above the double-ionization threshold. The results for the cross sections are compared with those obtained with state-of-the-art methods. The partial cross section for the photodetachment of H^- with the residual atomic hydrogen left in the $(\tilde{n}_1,\ell_1)$ state is given by

$$\sigma^{\tilde{n}_1 l_1} = \frac{2}{3}\pi^2\alpha\sum_{l_2} F_\Gamma^G, \quad (27)$$

where α is the fine-structure constant and F_Γ^G the oscillator strength either in the length gauge ($G\equiv L$) or in the velocity gauge ($G\equiv V$). These oscillator strengths are defined as follows:

$$F_\Gamma^L = 2\omega|\langle\Psi_{1S}^{0,0}|\hat{\epsilon}\cdot(\vec{r}_1+\vec{r}_2)|\Theta_\Gamma\rangle|^2, \quad (28)$$

$$F_\Gamma^V = \frac{2}{\omega}|\langle\Psi_{1S}^{0,0}|\hat{\epsilon}\cdot(\vec{\nabla}_1+\vec{\nabla}_2)|\Theta_\Gamma\rangle|^2. \quad (29)$$

In these expressions, ω is the photon frequency and it is assumed that the electric field is polarized linearly along the unit vector $\hat{\epsilon}$. $\Psi_{1S}^{0,0}$ is the ground state of H^- obtained by diagonalizing the atomic Hamiltonian (2) (with $Z=1$) in our finite basis and Θ_Γ the continuum P state associated with the channel Γ and evaluated within the J matrix method. Let us first consider photon energies below the double-ionization threshold. In these calculations, the Sturmian nonlinear parameter $k=0.9$. For $L=0$, 7 pairs (ℓ_1,ℓ_2) of electron angular momenta are included [(0,0),(1,1),…,(6,6)]; $1\leqslant n_1\leqslant 50$ and $1\leqslant n_2\leqslant 50$. In this way, the number of terms, N, in our expansion of the ground-state wave function of H^- is 8925 and its energy −0.527 73 a.u. to be compared with the best nonrelativistic value of 0.527 751 016 544 306 a.u. by Drake [51]. For $L=1$, we include six pairs (ℓ_1,ℓ_2): namely, (0,1), (1,2),…,(5,6); $1\leqslant n_1\leqslant 50$ and $1\leqslant n_2\leqslant 50$. The dimension of our finite basis in the inner region is 15 000, and the total number of channels included is 540. In Fig. 1, we show the partial cross sections for photodetachment of H^- for various photon energies in the region of the shape resonance just above the $n=2$ threshold; the residual hydrogen atom is left in its ground $(1s)$ or first excited $(2s,2p)$ states. Below the

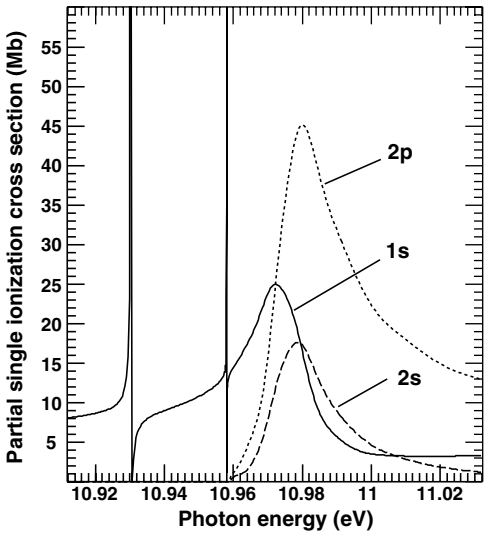

FIG. 1. Partial cross sections for photodetachment of H^- in the region of the shape resonance just above the $n=2$ threshold; the residual hydrogen atom is left in its ground $(1s)$ or the first excited $(2s,2p)$ states.

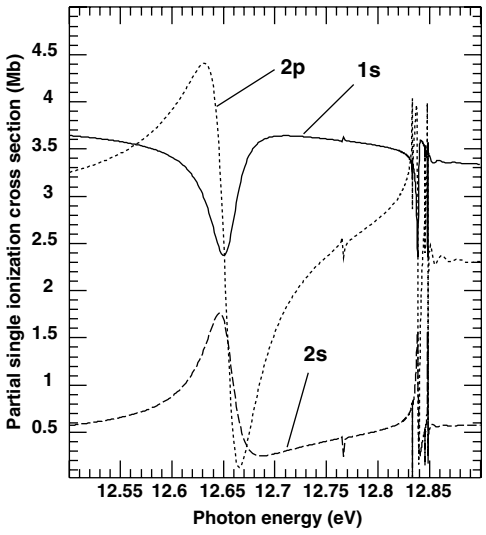

FIG. 2. Partial cross sections for photodetachment of H^- around the $n=3$ threshold; the residual hydrogen atom is left in its ground $(1s)$ or the first excited $(2s,2p)$ states.

$n=2$ threshold, the cross section for photodetachment to the $n=1$ channel exhibits a Feshbach resonance at a photon energy of 10.930 20 eV followed by an extremely narrow resonance at 10.958 002 eV and known as a "dipole resonance" [63]. It is produced by the dipole coupling between the degenerate $2s$ and $2p$ states of atomic hydrogen [64,65]. Above the $n=2$ threshold, around the shape resonance at about 10.98 eV, all partial cross sections exhibit a maximum. We have compared our results with those of Venuti and Decleva [60]. They build the continuum wave function via a least-squares solution of the Schrödinger equation and use a very large basis-set expansion based on B-spline radial functions within a general CI formulation. Below the $n=2$ threshold, there is a perfect agreement between their results and ours. Above the $n=2$ threshold, we observe small differences (less than 1%) in the partial cross sections. In fact, above the $n=2$ threshold, the continuum becomes multichannel with degenerate target states. This degeneracy induces a weak but long-range $1/r^2$ potential responsible for the sensitivity of the partial cross sections to the different channels coupling. In order to take into account this potential accurately within the J-matrix approach, we can either increase the size of the internal basis or introduce an intermediate region [66] between the internal and the asymptotic one in which we keep the first two terms of the multipole expansion of the $1/r_{12}$ potential. By increasing the size of the internal basis to 19 600 [4 pairs (ℓ_1,ℓ_2) and 70 Coulomb Sturmian functions per electron], our results now agree (to 3 significant digits) with the data of Venuti and Decleva [60]. In Fig. 2, we show the partial cross sections for photodetachment of H^- above the $n=3$ threshold. Our results are again in excellent agreement with those of Venuti and Decleva. In particular, we have checked by expanding the photon energy scale that the complicated structure of all partial cross sections around the $n=3$ threshold (photon energy around 12.85 eV) is correct. Let us now analyze the partial cross sections of one-photon SI above the double-ionization threshold. As far as we know, very few calculations have been performed in this frequency regime. Extremely accurate results very close to threshold (0.1 eV above) have been obtained recently by Bouri *et al.* [20] in He up to $n=50$ for the excitation level of the residual ion. Results for He and H^-, far from threshold, have been also obtained by Kheifets and Bray [16,67]. In both cases, however, no selection of the angular momentum of the final excited state of the residual ion has been made. In order to test the accuracy of our J-matrix approach in the most demanding case, H^-, we calculated the partial cross sections by means of a method developed by Proulx and Shakeshaft [68] which takes into account fully the correlation in the final state. They show that the amplitude of probability can be written as follows:

$$A_{fi}^{(\ell_1)} = \sqrt{2}(\langle \phi_{\ell_1,n_1}| \otimes \langle \psi^-_{\ell_2,\epsilon}|)\left(E_f^{(0)} - H + \frac{1}{r_{12}}\right)|F\rangle, \quad (30)$$

with

$$(E_i^{(0)} + \omega - H)|F\rangle = V_+|\psi_i\rangle. \quad (31)$$

$E_i^{(0)}$ and $E_f^{(0)}$ are the (field-free) unperturbed energies of the initial and final states while $V_+ = \frac{1}{2}A_0\vec{e}_z\cdot(\vec{\nabla}_1+\vec{\nabla}_2)$ describes the interaction of the atom with a linearly polarized electric field written in terms of the potential vector amplitude A_0. Note that Eq. (30) is exact although the final state is represented by a symmetrized direct product $\langle \phi_{\ell_1,n_1}| \otimes \langle \psi^-_{\ell_2,\epsilon}|$ of a given hydrogen bound state of principal quantum number n_1 and angular quantum number ℓ_1 with a pure Coulomb wave of energy ϵ that behaves asymptotically as an ingoing wave. In Fig. 3, we show our results for various partial cross sections of photodetachment of H^- as a function of the photon energy (above the double-ionization threshold). In our calculations, the Sturmian nonlinear parameter $k=0.9$ and 7 pairs (ℓ_1,ℓ_2) of electron angular momenta are taken into account with $1 \leqslant n_1,n_2 \leqslant 50$. Our J-matrix results are in very good

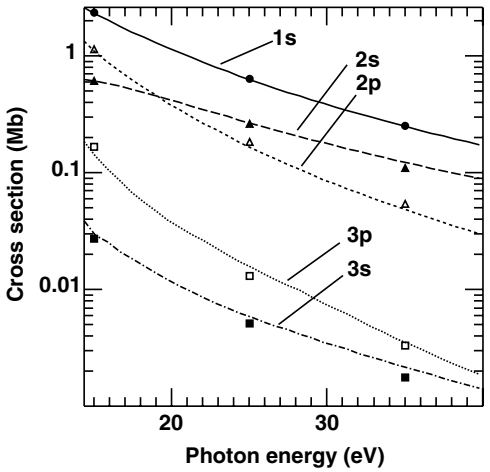

FIG. 3. Partial cross sections for photodetachment of H^- for photon energies above the double-ionization threshold. The residual hydrogen atom is left in its ground state ($1s$) and various excited states indicated in the figure. The lines correspond to the results obtained with the Proulx-Shakeshaft method. The dots, triangles, and squares at photon energy of 15 eV, 25 eV, and 35 eV are our J-matrix results.

agreement with those obtained by means of Eq. (30). There are, however, small differences at 35 eV attributed to the size of the basis we use in the internal region considered in our J-matrix approach. This last test shows that above the double-ionization threshold, the approximate description of the double-continuum channels improves with the size of the basis. We have checked that all the results presented here for photon energies both below and above the double-ionization threshold are gauge independent.

C. Time propagation

The TDSE for a two-electron system exposed to an oscillating field reads

$$i\frac{\partial}{\partial t}\Psi(\vec{r}_1,\vec{r}_2,t) = [H + D_G(t)]\Psi(\vec{r}_1,\vec{r}_2,t), \tag{32}$$

where H is the atomic Hamiltonian (2). $D_G(t)$ describes the dipole interaction of the system with the oscillating field either in the length gauge ($G \equiv L$) or in the velocity gauge ($G \equiv V$):

$$D_L(t) = \vec{E}(t)\cdot(\vec{r}_1 + \vec{r}_2), \tag{33}$$

$$D_V(t) = -i\vec{A}(t)\cdot(\vec{\nabla}_1 + \vec{\nabla}_2). \tag{34}$$

$\vec{E}(t)$ denotes the electric field and $\vec{A}(t) = \hat{z}A_0 f(t)\sin(\omega t)$ the corresponding vector potential which oscillates at the frequency ω and which is assumed linearly polarized along the z axis. $f(t)$ is the pulse envelope given by

$$f(t) = \cos^2(t/\tau) \quad (|t| \leq \pi\tau/2),$$

$$= 0 \quad (|t| > \pi\tau/2). \tag{35}$$

Note that $D_V(t)$ does not contain the $A^2(t)$ term since within the dipole approximation, this term is eliminated from the interaction Hamiltonian through a contact transformation of the wave function. The projection of the TDSE onto our basis [see Eq. (7)] leads to a system of first-order differential equations

$$i\frac{\partial}{\partial t}\mathbf{S}\Psi(t) = [\mathbf{H} + g(t)\mathbf{D}_G]\Psi(t), \tag{36}$$

where $\mathbf{D}_G$ is the matrix associated with the dipole operator in gauge G. $g(t)$ is a scalar function that equals $E_z(t)$ in the length gauge and $-iA_z(t)$ in the velocity gauge. $\Psi(t)$ is the vector representation of the wave function of the two-electron system in our basis. Due to the stiffness of the system (36) (see, for instance, [43]), it is necessary to switch to the atomic basis in which the atomic Hamiltonian (2) is diagonal. Upon this condition, the system (36) becomes

$$i\frac{\partial}{\partial t}\mathbf{\Phi}(t) = [\mathbf{h} + g(t)\mathbf{W}_G]\mathbf{\Phi}(t), \tag{37}$$

where $\mathbf{h}$ is a diagonal matrix containing the eigenvalues of the atomic Hamiltonian (2). $\mathbf{W}_G = \mathbf{P}^t\mathbf{V}^t\mathbf{D}_G\mathbf{V}\mathbf{P}$ and $\mathbf{\Phi}(t) = \mathbf{P}^t\mathbf{V}^{-1}\Psi(t)$. In these expressions, matrix $\mathbf{V}$ is given by Eq. (22) and the matrix $\mathbf{P}$ denotes the orthogonal matrix that diagonalizes $\tilde{\mathbf{H}}$ [see Eq. (19)]. In order to solve the system of equations (37), we use the interaction picture where the rapid oscillations due to the atomic energies are absorbed in the wave function by setting

$$\mathbf{\Phi}_I(t) = e^{i\mathbf{h}t}\mathbf{\Phi}(t), \tag{38}$$

where $\mathbf{\Phi}_I(t)$ is the vector associated with the time-dependent wave function in the interaction picture. The above transformation from the Schrödinger to the interaction picture requires some precautions when complex Coulomb-Sturmian bases are used or, equivalently, when a complex scaling of the total Hamiltonian is performed. Indeed, the imaginary part of the atomic energies brings overflows since the exponential in Eq. (38) becomes very large. In order to avoid such problems, we consider the following transformation:

$$\mathbf{\Phi}_I(t) = e^{i\mathbf{h}_r t}\mathbf{\Phi}(t), \tag{39}$$

where $\mathbf{h}_r$ denotes the real part of the diagonal matrix of atomic energies ($\mathbf{h} = \mathbf{h}_r + i\mathbf{h}_i$). Substituting Eq. (39) into Eq. (37) leads to

$$\frac{\partial}{\partial t}\mathbf{\Phi}_I(t) = [\mathbf{h}_i - ig(t)e^{+i\mathbf{h}_r t}\mathbf{W}_G e^{-i\mathbf{h}_r t}]\mathbf{\Phi}_I(t). \tag{40}$$

This equation is solved by means of an explicit method of Runge-Kutta type. We use an embedded formula [69] that allows an automatic control of the time step during the propagation.

In practice, our basis is truncated so that the resulting wave function represents a restricted region of space—say, a sphere of radius R_0. As long as the system remains in this sphere during the time the system interacts with the external field, the basis is adequate. However, if the system breaks up

during its evolution, as is the case when ionization occurs, some fragments may reach the surface of the sphere. If the basis is real, these fragments must reflect from the surface and return to the interior of the sphere. In the present case, this effect is more likely to occur for single ionization, leaving the residual ion (or atom) in its ground state since the outgoing electron is usually fast. These unphysical reflections are avoided by complex-scaling the total Hamiltonian since at large distances—i.e., at large time—the negative imaginary part of the continuum energies (above the first single-continuum threshold) induces a rapid damping of the corresponding components of the ionized wave packet (see, for instance, [70]), thereby simulating the presence of an absorber at the boundaries of the sphere. In the present calculations involving the *J*-matrix method, we use a real basis.

D. Observables

The total wave packet after the end of the time propagation reads

$$\Psi_{total} = \sum_{L} \sum_{\alpha} c_{\alpha} \Psi_{\alpha}^{L,M=0}, \tag{41}$$

where α runs over all atomic states of the system that are described in our Coulomb-Sturmian basis. The extraction of a quantitative information from this final wave packet constitutes the major problem of all time-dependent approaches. Since the time propagation is always performed over finite distances, one way to disentangle single- and double-ionization contributions is to project the final ionized wave packet after the interaction with the pulse, on the corresponding (fully correlated) multichannel wave function associated with the single or double continuum.

In order to calculate the single- and double-ionization probabilities, we proceed as follows. We first rewrite the total wave packet of the system after the interaction with the pulse, as a sum of two terms:

$$\Psi_{total} = \Psi_{BS} + \Psi_{C}, \tag{42}$$

where Ψ_{BS} and Ψ_{C} are the bound- and continuum-state components, respectively. Since the time propagation is performed in the atomic basis, the calculation of the bound-state component Ψ_{BS} of the total wave packet is straightforward. Ψ_{C} given by $\Psi_{total} - \Psi_{BS}$ is actually a linear superposition of single- and double-continuum multichannel scattering wave functions. In order to extract the single-continuum component Ψ_{SC} from Ψ_{C}, we write

$$\Psi_{SC} = \sum_{\Gamma} \int_{E_i}^{\infty} \langle \Psi_C | \Theta_{\Gamma}(E) \rangle \Theta_{\Gamma}(E) dE, \tag{43}$$

where $\Theta_{\Gamma}(E)$ is the scattering state generated by the *J*-matrix method [see Eq. (24)] and normalized in the energy space. Γ refers to a given channel of single ionization and E is the total energy of the system. E_i is the first single-ionization threshold. Therefore, the partial (in a given channel) and total SI probability densities are given by

$$\left(\frac{dP_{SI}}{dE} \right)_{\Gamma} = |\langle \Psi_C | \Theta_{\Gamma}(E) \rangle|^2, \tag{44}$$

$$\left(\frac{dP_{SI}}{dE} \right)_{total} = \sum_{\Gamma} |\langle \Psi_C | \Theta_{\Gamma}(E) \rangle|^2. \tag{45}$$

In order to calculate the double-continuum component Ψ_{DC}, we could project Ψ_{C} on the multichannel wave functions associated to all double-continuum channels. Each double-continuum channel is characterized by both the (discretized) energy associated to the pseudostate that describes the inner electron and to the energy of the outer electron. The calculation of the double-continuum component requires integration on all possible values of the energies of both electrons. Instead of proceeding in this way, it is easier to calculate the double-continuum component Ψ_{DC} by substracting both Ψ_{BS} and Ψ_{SC} from the total wave packet Ψ_{total}. The total DI probability is then obtained as follows:

$$P_{DI} = \int \int d\vec{r}_1 d\vec{r}_2 (|\Psi_{total} - \Psi_{BS} - \Psi_{SC}|^2). \tag{46}$$

The accuracy of this expression relies on the fact that the scattering states $\Theta_{\Gamma}(E)$ are orthogonal (by construction) to the other eigenstates of the atomic Hamiltonian. Note that the total DI probability P_{DI} is also obtained by writing

$$P_{DI} = \sum_{\beta} |c_{\beta}|^2 - \sum_{\Gamma} \int_{E_i}^{\infty} dE \left(\frac{P_{SI}}{dE} \right)_{\Gamma}, \tag{47}$$

where the sum over β—i.e., over the atomic states described in our Coulomb-Sturmian basis—is restricted to the states whose energy is larger or equal to the energy of the first single-ionization threshold. Both expressions (46) and (47) are formally equivalent. From the numerical point of view, however, they differ significantly. In all the calculations that will be presented in the next sections, we have checked that the relative difference between the results obtained from these two expressions is less than 10^{-4}.

The present time-dependent approach can also be used to calculate generalized cross sections. It is, however, necessary to define under what conditions this can be done. First, it is important to remember that generalized cross sections are defined in terms of a transition amplitude that is calculated at the lowest nonvanishing order of perturbation theory. This means that within our time-dependent approach, the peak intensity of the external field must be sufficiently low to avoid contributions from higher-order transitions (involving more photons). Second, it is possible to define a generalized cross section only if the transition is direct. In the case of multiphoton double ionization, however, the transition from the initial to the final state may be sequential: a single ionization of the atom followed by a single ionization of the residual ion in a given state. In that case, the transition probability varies quadratically with the interaction time, preventing the definition of a time-independent rate. These two preliminary remarks introduce some limitations regarding the reliability of a time-dependent approach to provide accurate information on the generalized cross sections. For the sake of illustration, let us consider two-photon double ionization of He. If the photon energy is less than 2 a.u. (which corresponds to the minimal energy required to ionize He^+ with one photon from its ground state), the process is essentially

direct. However, it is possible to reach the double continuum via two sequential three-photon transitions

$$\mathrm{He} + h\nu \rightarrow [\mathrm{He}^{+}(1s) + e^{-}] + 2h\nu \rightarrow (\mathrm{He}^{2+} + 2e^{-}),$$

$$\mathrm{He} + 2h\nu \rightarrow (\mathrm{He}^{+*} + e^{-}) + h\nu \rightarrow (\mathrm{He}^{2+} + 2e^{-}).$$

Note that depending on the photon energy, the second step of the first of these two sequential transitions may be resonant. Within a time-dependent approach, all these direct and sequential transitions are taken into account, so in order to calculate the direct two-photon double ionization, it is important to make sure that both sequential transitions are negligible—i.e., far from saturation—in particular, near resonance. It is therefore necessary to work at sufficiently low field intensities.

Upon these conditions, the N-photon transition probability per unit of time—i.e., the N-photon rate Γ_N—reads

$$\Gamma_N = \sigma_N \Phi^N, \tag{48}$$

where σ_N is the corresponding generalized cross section and Φ the photon flux given (in a.u.) by I/ω where I is the intensity of the field whose amplitude is assumed constant for the time being. In the case of a pulse, we use the adiabatic approximation to obtain the following expression for the N-photon transition probability P_N:

$$P_N = \int_{-\infty}^{\infty} dt \Gamma(t) = \sigma_N \int_{-\infty}^{\infty} dt \Phi^N(t). \tag{49}$$

The generalized cross section σ_N is deduced from this expression. Let us consider a cosine square pulse [see expression (35)] whose total duration is n optical cycles. We denote the pulse peak intensity in Watt/cm^2 by I_0 and the photon energy in eV by E_{photon}. If P_1 and P_2 give the probability of a given one-photon and two-photon process respectively, the corresponding generalized cross sections in their appropriate units are written

$$\sigma_1[cm^2] = 1.032 \times 10^{-4} \frac{E_{photon}^2 P_1}{nI_0}, \tag{50}$$

$$\sigma_2[cm^4 s] = 2.28 \times 10^{-23} \frac{E_{photon}^3 P_2}{nI_0^2}. \tag{51}$$

In principle, the generalized cross section should be independent of n, the total number of optical cycles within the pulse. In practice, however, since our real basis is finite, the reflection problem imposes some limitations on the duration of the pulse and therefore on the size of our Coulomb-Sturmian basis. Irrespective of this reflection problem, the choice of the parameter n is directly related to the validity of the adiabatic approximation. In general, pulses of a few cycles are sufficient [71] except when some intermediate or final states are resonant. In the latter case, long pulses are necessary, making our time-dependent approach less appropriate.

The previous discussion raises the following question: is it possible within our time-dependent approach to extrapolate our results to infinite pulse durations? In order to answer to that question, let us consider a one-photon transition from a bound state ϕ_{bs} to a continuum ψ_{cont} of states. It is shown in many textbooks on quantum mechanics that the probability of such a transition as a function of the interaction time T (i.e., the pulse duration) is written:

$$P(T) = \int_{E_{threshold}}^{\infty} K(E_f - E, T) |\langle \phi_{bs} | D | \psi_{cont}(E) \rangle|^2 \rho(E) dE. \tag{52}$$

$E_{threshold}$ is the lower bound of the continuum energy, and $K(E-E_f,T)$ is a kernel that depends on the pulse shape. $\langle \phi_{bs} | D | \psi_{cont}(E) \rangle$ is the dipole matrix element between the initial bound state and the continuum state of energy E, and $\rho(E)dE$ is the density of final states within the energy interval $[E, E+dE]$. In the case of the cosine square pulse (35), the kernel is written:

$$K(E - E_f, T) = \frac{4\pi^4 \sin^2[(E - E_f)T/2]}{(E - E_f)^2 [T^2 (E - E_f)^2 - 4\pi^2]^2}. \tag{53}$$

For $E = E_f \pm 2\pi/T$ this kernel is well defined. For long pulse durations T, it is strongly peaked around $E=E_f$, thereby reinforcing energy conservation. In fact, since in the limit $T \rightarrow \infty$,

$$\frac{\sin^2[(E - E_f)T/2]}{(E - E_f)^2} \approx \frac{\pi}{2} T \delta(E - E_f), \tag{54}$$

we obtain the following expression for the transition rate (Fermi's golden rule):

$$\Gamma = \frac{dP(T)}{dT} = |\langle \phi_{bs} | D | \psi_{cont} \rangle|^2 \rho(E_f). \tag{55}$$

Note that in writing the above expression, it is assumed that all angular integrations have been performed. This result means that for a given energy E, the cross section we are looking for is directly proportional to $F(E) = |\langle \phi_{bs} | D | \psi_{cont}(E) \rangle|^2 \rho(E)$. Now, instead of considering very long pulses, we could calculate $P(T)$ either for various finite values of T and a fixed value of the photon energy or a fixed value of T and various values of the photon energy. $F(E)$ is then an unknown function of E, a solution of the integral equation (52). It turns out, however, that this integral equation is extremely hard to solve, therefore making the extrapolation procedure difficult. As a matter of fact, the technique we found the most accurate to solve this equation consists simply in approximating $F(E)$ by $F(E_f)$ so that it can be factorized out. This is because even for short pulse durations T, the kernel still exhibits a sharp peak [72] at the conservation of energy $E=E_f$. In this way, we obtain a relation between $P(T)$ and $F(E)$ that leads to expression (50) for the corresponding cross section. This procedure, however, does not work in two particular cases: (i) close to threshold where nonadiabatic effects become important and (ii) when the final state lies near a resonance because $F(E)$ varies too rapidly around $E=E_F$. In this latter case, it is necessary to use much longer pulses, thereby exposing our procedure to the reflection problem. It is interesting to point out that our results for the direct double-ionization cross section are much less sen-

sitive to the duration of the pulse we use to perform the calculations than in the case of single ionization. In fact, since the reflection problem occurs essentially in the single-ionization channels, we "eliminate" its effect by substracting the singly ionized wave packet from the total wave packet (single ionization is only described in these two wave packets). Finally, we would like to finish this section with two remarks. First, the present approach does not allow an accurate calculation of the differential cross sections (energy and angular distributions). This point will be addressed in a forthcoming publication. Second, the fact that the J-matrix method requires the use of only one nonlinear parameter in our Coulomb-Sturmian basis does not prevent us from considering various sets of nonlinear parameters in the case of the time propagation.

III. RESULTS

In the first part of this section, we focalize on one-photon SI and DI of He and H^-. Our objective is to check the accuracy of our time-dependent approach by comparing our results for the total cross section to those obtained by state-of-the-art methods. We then apply our approach to two-photon double ionization of He.

A. One-photon double ionization of He and H^-

Let us first consider the one-photon double ionization of He. In our calculations, three values (0, 1, and 2) of the total angular momentum L are included. For $L=0$, four pairs (ℓ_1,ℓ_2) of electron angular momenta are taken into account $[(0, 0),\ldots,(3, 3)]$ while for $L=1$ and 2, three pairs are included $[(0, 1), (1, 2), (2, 3)]$ and $[(1, 1), (0, 2), (1, 3)]$, respectively. For all pairs of electron angular momenta (ℓ_1,ℓ_2), we use the same set (2.0, 60, 2.0, 60) of Coulomb-Sturmian functions. The peak intensity of the pulse is equal to 10^{13} W/cm^2. The convergence of the results for the total SI and DI cross sections has been checked as a function of the pulse duration. In the present case, we used a pulse whose total duration varies from 6 to 20 optical cycles. The gauge invariance (length and velocity) of our results has also been checked. The total double-ionization cross section as a function of the excess photon energy is shown in Fig. 4. Our TDSE results that take into account fully the final-state correlation are in very good agreement with both the experimental data of Samson *et al.* [73] and with the results of Proulx and Shakeshaft [13] who used the so-called flux formula. We also compare our results with TDSE results in which we project the final wave packet in the Schrödinger picture on a direct (uncorrelated) product of Coulomb waves of effective charge $Z=2$. These latter data are slightly below the other curve except at high photon energy where the final-state electron correlation is not expected to contribute significantly. Instead of analyzing the SI cross section we study, in Fig. 5, the ratio of double-to-single one-photon ionization. Such a ratio is in general more sensitive to the type of approach that is used to calculate both SI and DI cross sections. Our TDSE fully correlated results are again in perfect agreement with both the experimental data of Samson *et al.* [73]

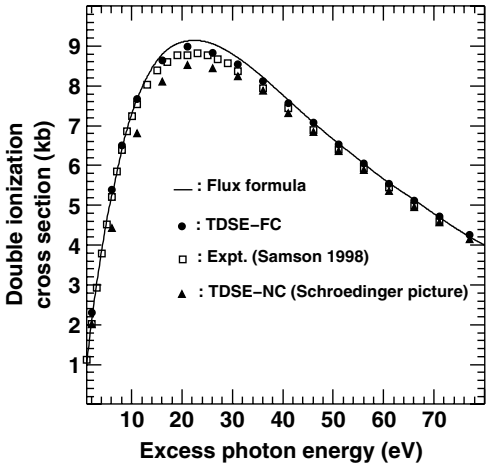

FIG. 4. Total cross section in Kb of one-photon double ionization of He as a function of the excess photon energy in eV. The solid line has been obtained by means of the flux formula [13]. The solid circles are our TDSE results that take fully into account the electron correlation in the final state. The squares are the experimental results of Samson *et al.* [73]. The solid triangles are our TDSE results obtained by projecting the final wave packet in the Schrödinger picture on a direct (uncorrelated) product of Coulomb functions of effective charge $Z=2$.

and the theoretical data of Proulx and Shakeshaft [13].

Let us now consider H^-. In this case, electron-electron correlations play a crucial role. It is therefore not surprising that important discrepancies still subsist between the results of all existing theoretical approaches. In our calculations, we take into account 3 values of the total angular momentum L (0, 1, and 2). For $L=0$, we considered 4 pairs (ℓ_1,ℓ_2) of electron angular momenta [(0,0), (1,1), (2,2), and (3,3)]. For $L=1$ and 2, we used 3 pairs of electron angular momenta [(0,1),(1,2),(2,3)] and [(0,2),(1,1),(1,3)], respectively. In all cases, we use the following set (1.0,60,1.0,60) of Coulomb-Sturmian functions. All calculations have been performed

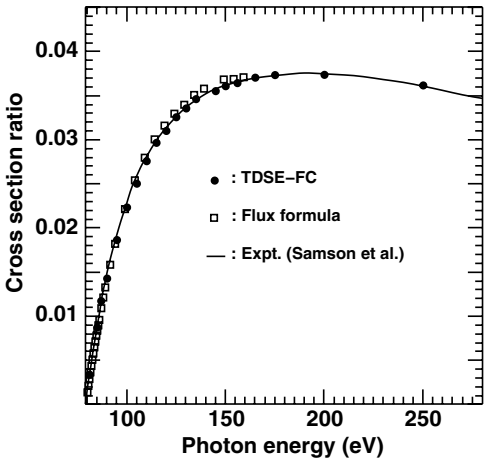

FIG. 5. The ratio of double-to-single one-photon ionization cross sections in He as a function of the photon energy in eV. The solid line is a fit of the experimental data of Samson *et al.* [73]. The squares are the results of Proulx and Shakeshaft by means of the flux formula [13]. The dots are our TDSE fully correlated results.

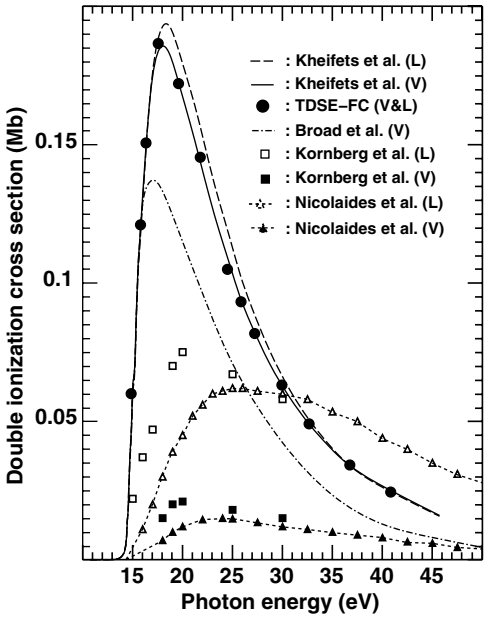

FIG. 6. Total cross section in Mb of one-photon double ionization of H^- as a function of the photon energy in eV. The solid and dashed curves are the results of Kheifets and Bray [16] in the velocity and length gauges, respectively. The black dots are our TDSE fully correlated and gauge-invariant results. The dot-dashed curve is the result of the *J*-matrix calculation of Broad and Reinhardt [62] in the velocity gauge. The open and solid squares are the results of Kornberg and Miraglia [74] in the length and velocity gauges, respectively. The open and solid triangles are the results of Nicolaides *et al.* [75] in the length and velocity gauges, respectively.

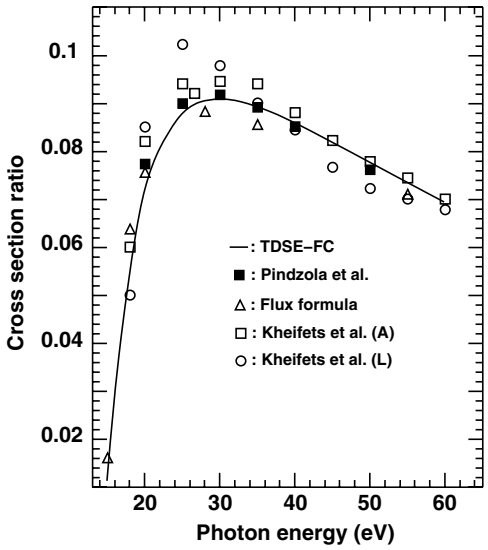

FIG. 7. The ratio of double-to-single one-photon ionization cross sections in H^- as a function of the photon energy in eV. The solid line is our TDSE fully correlated and gauge-invariant results. The open squares and circles are the CCC results of Kheifets and Bray [16] in the acceleration and the length gauges, respectively. The open triangles refer to the results obtained by means of the flux formula of Proulx and Shakeshaft [13]. The solid squares are the TDSE results of Pindzola and Robicheaux [76] with an uncorrelated final state.

with a peak intensity of 10^{11} W/cm^2 and pulses whose total duration varies from 8 to 20 optical cycles. In Fig. 6, we show the one-photon DI total cross section. Our TDSE fully correlated and gauge invariant results are in perfect agreement with the CCC results of Kheifets and Bray [16] in the velocity gauge. Their results in the length gauge are slightly higher in the vicinity of the maximum. In the *J*-matrix calculations of Broad and Reinhardt [62], the double continuum is described asymptotically by an appropriately symmetrized product of a plane wave and a set of pseudostates for the "internal" electron. This description is clearly an approximation. However, their results obtained with a relatively small basis and within the velocity gauge are not in too bad disagreement with the CCC or with our TDSE results. The variational configuration-interaction calculations of Nicolaides *et al.* [75] as well as the calculations of Kornberg and Miraglia [74] based on the BBK function for the description of the double continuum, differ significantly from all other results and are strongly gauge dependent. As expected, discrepancies are also important in the case of the ratio of double-to-single one-photon ionization cross section shown in Fig. 7. At high photon energy, our TDSE fully correlated results are in good agreement with the CCC results of Kheifets and Bray [16] in the acceleration gauge. Their results in the length gauge, however, differ significantly. It is important to note that Kheifets and Bray used a very good ground state of H^- in their calculations: namely, a Hylleraas wave function with 20 nonlinear parameters. The results obtained with the flux formula of Proulx and Shakeshaft [13] are in fair agreement with ours. Surprisingly, the best agreement with our results occurs with TDSE results of Pindzola and Robicheaux in which the final state is uncorrelated. It is interesting at this stage to discuss in detail this approximation, which consists in projecting the final ionized wave packet on the direct (uncorrelated) product $|\psi^-_{\epsilon_1}\rangle \oplus |\psi^-_{\epsilon_2}\rangle$ appropriately symmetrized. $|\psi^-_{\epsilon}\rangle$ represents an electron of energy $\epsilon > 0$ moving in the Coulomb potential $-Z/r$. The superscript $^-$ refers to the asymptotic ingoing-wave behavior of the corresponding Coulomb wave function $\langle \psi^-_{\epsilon} | \vec{r} \rangle$. The fact that this direct product of Coulomb states does not represent an eigenstate of the atomic Hamiltonian (2) has important consequences. First, the ionization probability depends on the picture (Schrödinger or interaction) used to describe the final ionized wave packet:

$$|\langle \psi^-_{\epsilon_1}| \oplus \langle \psi^-_{\epsilon_2}|\Phi_{sch}\rangle|^2 \neq |\langle \psi^-_{\epsilon_1}| \oplus \langle \psi^-_{\epsilon_2}|\Phi_I\rangle|^2, \qquad (56)$$

where $|\Phi_{sch}\rangle$ and $|\Phi_I\rangle$ are the final wave packet in the Schrödinger and interaction pictures respectively. Moreover, in contrast to the interaction picture, the modulus square of the projection of $|\Phi_{sch}\rangle$ on the direct product $|\psi^-_{\epsilon_1}\rangle \oplus |\psi^-_{\epsilon_2}\rangle$ keeps varying as the time evolves after the end of the pulse. This variation with time which is a consequence of the free evolution of $|\Phi_{sch}\rangle$ is in fact artificial. It manifests only because the final wave packet $|\Phi_{sch}\rangle$ is projected on a nonstationary state of the atomic Hamiltonian (2). Contrary to what Colgan *et al.* [26] claim, we think that it does not make sense to "wait" a few cycles after the end of the pulse that the system "relaxes" or in other words that the electron electron

correlation dies out before projecting $|\Phi_{sch}\rangle$ on the direct product of Coulomb states. In addition, it is important to stress that the final wave packets $|\Phi_{sch}\rangle$ and $|\Phi_I\rangle$ contain single-ionization components. As a result, its projection on the direct product $|\psi^-_{\epsilon_1}\rangle \oplus |\psi^-_{\epsilon_2}\rangle$ necessarily contains a contribution from single ionization because the direct product of Coulomb states is not orthogonal to actual continuum states of the atom. This effect is particularly important in the case of one-photon double ionization of He or H^- because the probability of single ionization is actually two orders of magnitude higher than the double-ionization probability. All these points are illustrated in Fig. 8 in the case of the one-photon DI of He and in Fig. 9 for H^-. In Fig. 8(a), we compare our TDSE fully correlated results for the one-photon DI of He with those obtained by projecting at the end of the pulse, the final wave packet in both the Schrödinger and interaction pictures on an uncorrelated product of Coulomb waves with the effective charge $Z=2$. At first sight, the Schrödinger picture seems to give very good results. However, these results change when the projection is performed some time after the end of the pulse. This is particularly true in the vicinity of the maximum of the cross section. We have checked that in some cases the corresponding maximum may be above our TDSE fully correlated results. On the other hand, there is no physical reason to privilege the Schrödinger picture with respect to the interaction picture. In principle, the calculation must be picture independent as is the case when we use a fully correlated final state. Within our approach, we can isolate both the singly ionized and doubly ionized wave packets from the total wave packet in a given picture. By projecting each of these wave packets on the direct product of Coulomb waves, we actually extract the SI component of the DI cross section. In Fig. 8(b), we consider the interaction picture. It is clear that the contribution from single ionization is rather significant in particular around the maximum. Similar results are obtained in the Schrödinger picture. Far from the maximum—i.e., for higher photon energies—the single-ionization component becomes quickly very small. In that case, the two electrons emerge from the reaction zone with a higher energy so that the product of two Coulomb waves becomes a better approximation of the actual double-continuum wave function. In the case of H^-, the role of the final-state correlation is even more important. In Fig. 9 we show the cross section of one-photon DI of H^- and compare our TDSE fully correlated results with those obtained by projecting the final wave packet both in the Schrödinger and interaction pictures on a product of Coulomb waves with effective charge $Z=1$. It is clear that, in the vicinity of the maximum and irrespective of the picture, the absence of final-state correlation is not a good approximation. This is, however, not true any more at higher photon energy like in the case of He. Note that our TDSE results in the Schrödinger picture with no correlation in the final state are in perfect agreement with those of Pindzola and Robicheaux [76].

B. Two-photon double ionization of He

Let us now consider the two-photon DI of He in a frequency regime where this process is direct—i.e., for photon energies less than 2 a.u., that is the energy required to photoionize $He^+(1s)$. In our calculations, we took into account four values of the total angular momentum L (0–3). For $L=0$, four pairs (ℓ_1,ℓ_2) of electron angular momenta $[(0,0),\ldots,(3,3)]$ are included, and for each of these pairs, we use the set (2.0,70,2.0,70) of Coulomb-Sturmian functions. For $L=1$, three pairs $[(0,1), (1,2)$ and $(2,3)]$ of electron angular momenta are included. In each case, we use the set

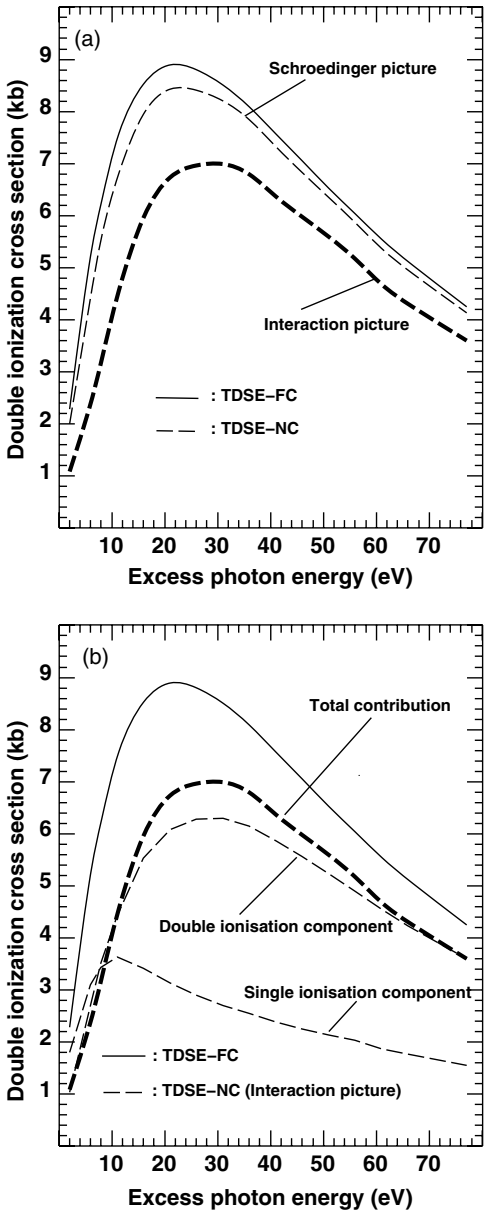

FIG. 8. Total cross section in Kb of one-photon double ionization of He as a function of the photon energy in eV. In (a), we compare our TDSE fully correlated results (solid line) with those obtained by projecting the final wave packet in the Schrödinger or in the interaction picture (dashed lines) on an uncorrelated product of Coulomb waves with the effective charge $Z=2$. In (b), the dashed lines refer to the results obtained by projecting either the final ionized wave packet, the final singly ionized wave packet, or the doubly ionized wave packet on the uncorrelated product of Coulomb waves. These results are compared to our TDSE fully correlated results (solid line).

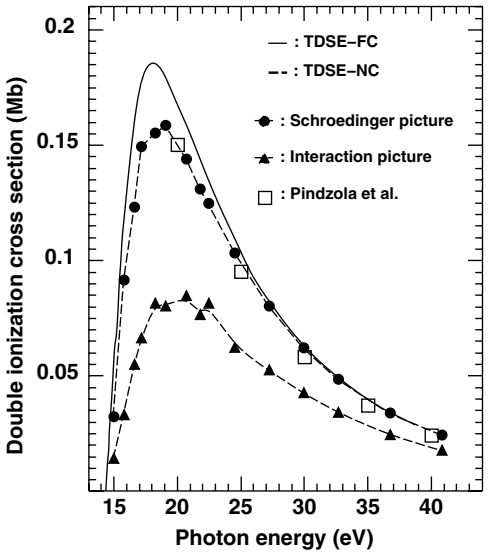

FIG. 9. Total cross section in Mb of one-photon double ionization of H^- as a function of the photon energy in eV. We compare our TDSE fully correlated results (solid line) with those (dashed lines) obtained by projecting the final wave packet in the Schrödinger (solid circles) or in the interaction picture (solid triangles) on an uncorrelated product of Coulomb waves with the effective charge $Z=1$. The solid squares refer to TDSE results of Pindzola et Robicheaux [76] who used an uncorrelated final state.

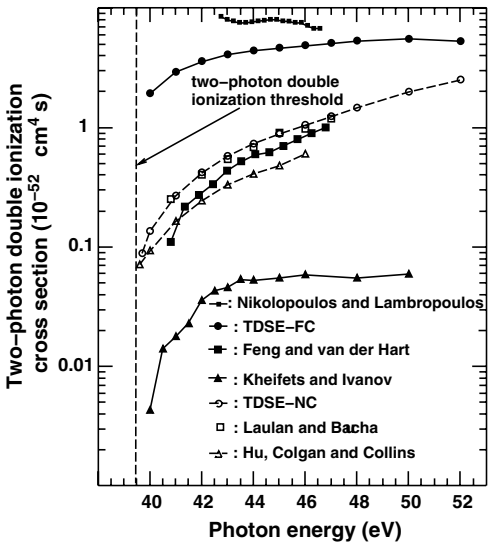

FIG. 10. Generalized cross section in cm^4 s of two-photon double ionization of He as a function of the photon energy in eV. The solid line with solid circles refer to our TDSE fully correlated results. The small solid squares are the results of Nikolopoulos and Lambropoulos [7]. The solid line with open circles are our TDSE results without electron correlation in the final state. The open squares are the TDSE results of Laulan and Bachau [30,37] with no correlation in the final state. The solid line with large solid squares are the *R*-matrix Floquet results of Feng and van der Hart [22] with some correlation in the final state. The dashed line with open triangles are the TDSE calculations of Hu, Colgan, and Collins [28] with no correlation in the final state. The solid line with solid triangles are the CCC results of Kheifets and Ivanov [17].

(1.6,60,1.2,120) of Coulomb-Sturmian functions. For $L=2$, four pairs of electron angular momenta [(0,2), (1,1), (1,3), and (2,2)] are considered with for each pair, the set (2.0,70,2.0,70) of Coulomb-Sturmian functions. Finally, for $L=3$, we included three pairs [(0,3),(1,2), and (1,4)] of electron angular momenta with the set (2.0,40,2.0,40) of Coulomb-Sturmian functions. We included the $L=3$ contribution because we have to make sure that the contribution of the two sequential channels mentioned before and that lead to the double-electron ejection is negligible. We considered two peak intensities 10^{11} W/cm^{13} and 10^{13} W/cm^2 and checked that the results for the generalized cross section are intensity independent. Most of the calculations have been performed with pulses of ten optical cycle (total duration). We also checked for a few photon energies that the results are stable as a function of the pulse duration. The generalized two-photon DI cross section as a function of the photon energy is presented in Fig. 10 where we compare our data with the other existing ones. At first sight, it is clear that the results depend strongly upon the way electron correlation is treated in the final state. For sufficiently low photon energies, our TDSE fully correlated results are systematically one order of magnitude higher than the other TDSE results [28,30,37] in which no correlation is included in the final state. On the other hand, our TDSE fully correlated results are of the same order of magnitude as the results of Nikolopoulos and Lambropoulos [7] who introduced correlation in the final state. They however differ significantly from the *R*-matrix Floquet results of Feng and van der Hart [22] who took, at least approximately, electron correlation into account in their calculations. Our results also differ by two order of magnitude from the CCC results of Kheifets and Ivanov [17]. It is worth noting that these CCC results are perturbative (in the external field) and that the sum over the intermediate states has been carried out by means of the closure approximation. This might explain the important difference in magnitude with our results. However, it is important to mention the agreement in shape between the CCC and our results. The convergence of our calculations has been checked as a function of the size of our radial and angular basis. It is worth mentioning that when we "switch off" the electron correlation in our *J*-matrix calculation of the multichannel continuum wave function, we remove both the radial and angular couplings between these channels. As a result, the SI probability increases by about 30% leading to a corresponding decrease of the DI probability. In that case, our results for the generalized DI cross section practically coincide with those obtained by projecting the final wave packet directly on an uncorrelated product of Coulomb waves (with $Z=2$). In fact, it is essentially the radial coupling between various channels of single ionization that gives rise to the strong effect observed in the SI generalized cross section. However, further investigations and, in particular, differential cross sections are needed to get a clear physical picture of the two-photon DI process. Finally, let us mention that there is one experimental data [77] for He at a photon energy of 41.8 eV. However, the uncertainty in particular on the field intensity and the fact that at this photon energy the various three-photon sequential transitions we mentioned before may

contribute prevents us from drawing conclusions regarding the validity of our results.

IV. CONCLUSION

In this contribution, we presented a numerical approach aimed at solving in its full dimensionality, the time-dependent Schrödinger equation that governs the interaction of a short, high-frequency electric field with a two-active-electron atomic system. Our objective is the study of the electron correlation in the *multiphoton* single ionization (with or without excitation of the residual ion) as well as double ionization of atoms.

Our approach is made up of three distinct steps. We first use a spectral method of configuration interaction type to build up the eigenstates of the atomic Hamiltonian. Second, we time propagate the total wave packet of the atom. Finally, we use the so-called *J*-matrix method to generate the continuum states on which we project the final wave packet to extract reliable information regarding single and double ionization. The spectral method consists in expanding the atomic eigenfunctions in a basis of symmetrized products of complex Coulomb-Sturmian functions of the electron radial coordinates and bipolar harmonics of the angular coordinates. We have shown that a single diagonalization of the atomic Hamiltonian in this basis provides a very accurate value of the energy of many singly and doubly excited states, the accuracy increasing while approaching the various single-ionization thresholds. The only relative weakness of this approach concerns the accuracy of the atomic ground-state energy, which is limited because the Kato cusp condition at a point where both electrons are "localized" is not satisfied. It is, however, important to stress that the accuracy we obtain for the ground-state energy (five digits) suffices for our purpose. The time propagation is performed in the atomic basis and within the interaction picture by means of an explicit Runge-Kutta embedded formula that allows an automatic control of the time step. The *J*-matrix method is used to generate the multichannel continuum (scattering) wave function. By projecting the final atomic wave packet on these functions, we obtain the singly ionized wave packet and, by substraction, the doubly ionized wave packet. This leads to the probability of single (with or without excitation of the residual ion) as well as double ionization of the atom. This substraction procedure relies on the fact that the single-continuum component of the continuum wave function calculated by the *J*-matrix method is sufficiently accurate. This accuracy of the *J*-matrix approach has been tested successfully in the case of one-photon ionization of H^-. Besides, we have also shown that our approach can be used to calculate single- and double-ionization cross sections. This is only true, however, in the following conditions: the ionization process is dominantly direct and the final continuum state is not too close to a resonance. At the present stage, however, our time-dependent approach does not provide reliable information on the electron angular and energy distributions.

The whole approach has been tested in the case of the one-photon single and double ionization of He and H^- where other sophisticated methods have provided very accurate data. We have shown that our results are in very good agreement with these data. Besides, we have tried to analyze the role of the electron correlation in the final state. Within our approach, however, the answer to this question is somehow ambiguous. Indeed, we show that projecting the final wave packet on an uncorrelated double-continuum wave function represents a serious approximation due to the fact that the uncorrelated final state is not an eigenstate of the atomic Hamiltonian. On the one hand, the result is strongly picture dependent and, on the other hand, irrespective of the picture, the projection of the final wave packet on this uncorrelated double-continuum wave function necessarily contains a single-ionization component that can be significant at low photon energy.

Our approach has been used to calculate the direct two-photon double-ionization cross section in He. Our results clearly demonstrate the importance of the electron-electron correlation in the final state. Further investigations, in particular an accurate calculation of the differential cross sections, are needed in order to elucidate the actual role of the electron-electron correlation in this direct two-photon process.

ACKNOWLEDGMENTS

One of us (G.L.K.) thanks the Laboratoire de Physique Atomique, Moléculaire et Optique (unité PAMO) of the Université Catholique de Louvain, for hospitality and financial support. The authors thank the Université Catholique de Louvain for providing them with an access to the supercomputer of the CISM (Centre de calcul Intensif et Stockage de Masse) which is supported by the FNRS (Fonds National de la Recherche Scientifique) through the FRFC (Fonds de la Recherche Fondamentale et Collective) project No. 2.4556.99, "Simulations numériques et traitement des données". The authors are indebted to Henri Bachau, Peter Lambropoulos, Laurence Malegat, Armin Scrinzi, and Robin Shakeshaft for many excellent suggestions and interesting discussions. They also thank J. Colgan, A. Kheifets, and H. van der Hart for sending them their theoretical data.

[1] R. Wehlitz, I. A. Sellin, O. Hemmers, S. B. Whitfield, P. Glans, H. Wang, D. W. Lindle, B. Langer, N. Berrah, J. Viefhaus, and U. Becker, J. Phys. B **30**, L51 (1997).

[2] R. Dörner, J. M. Feagin, C. L. Cocke, H. Bräuning, O. Jagutzki, M. Jung, E. P. Kanter, H. Khemliche, S. Kravis, V. Mergel, M. H. Prior, H. Schmidt-Böcking, L. Spielberger, J. Ullrich, M. Unversagt, and T. Vogt, Phys. Rev. Lett. **77**, 1024 (1996).

[3] J. R. Harries, J. P. Sullivan, S. Obara, P. Hammond, and Y. Azuma, J. Phys. B **36**, L319 (2003); J. R. Harries, J. P. Sulli-

van, S. Obara, Y. Azuma, J. G. Lambourne, F. Penent, R. I. Hall, P. Lablanquie, K. Bucar, M. Zitnik, and P. Hammond, *ibid.* **38**, L153 (2005).
[4] H. Bräuning, R. Dörner, C. L. Cocke, M. H. Prior, B. Krässig, A. S. Kheifets, I. Bray, A. Bräuning-Demian, K. Carnes, S. Dreuil, V. Mergel, P. Richard, J. Ullrich, and H. Schmidt-Böcking, J. Phys. B **31**, 5149 (1998).
[5] P. M. Paul, E. S. Toma, P. Breger, G. Mullot, F. Augé, Ph. Balcou, H. G. Muller, and P. Agostini, Science **292**, 1689 (2001).
[6] J. Andruszkow *et al.*, Phys. Rev. Lett. **85**, 3825 (2000).
[7] L. A. A. Nikolopoulos and P. Lambropoulos, J. Phys. B **34**, 545 (2001).
[8] M. R. H. Rudge, and M. J. Seaton, Proc. R. Soc. London, Ser. A **283**, 262 (1965); M. R. H. Rudge, Rev. Mod. Phys. **40**, 564 (1968); R. K. Peterkop, *Theory of Ionization of Atoms by Electron Impact* (Colorado Associate University Press, Boulder, 1977).
[9] F. W. Byron and Ch. J. Joachain, Phys. Rev. **164**, 1 (1967).
[10] M. Brauner, J. S. Briggs, and H. Klar, J. Phys. B **22**, 2265 (1989).
[11] F. Maulbetsch and J. S. Briggs, J. Phys. B **26**, 1679 (1993); J. Phys. A **26**, L647 (1993); J. Phys. A **27**, 4095 (1994).
[12] M. Pont, R. Shakeshaft, F. Maulbetsch, and J. S. Briggs, Phys. Rev. A **53**, 3671 (1996).
[13] D. Proulx and R. Shakeshaft, Phys. Rev. A **48**, R875 (1993).
[14] M. Pont and R. Shakeshaft, Phys. Rev. A **51**, 494 (1995).
[15] R. Shakeshaft, Phys. Rev. A **60**, 1280 (1999).
[16] A. S. Kheifets and I. Bray, Phys. Rev. A **58**, 4501 (1998).
[17] A. S. Kheifets and I. A. Ivanov, J. Phys. B **39**, 1731 (2006); I. A. Ivanov and A. S. Kheifets, Phys. Rev. A **71**, 043405 (2005).
[18] P. J. Marchalant and K. Bartschat, Phys. Rev. A **56**, R1697 (1997).
[19] L. Malegat, P. Selles, and A. K. Kazansky, Phys. Rev. Lett. **85**, 4450 (2000); A. K. Kazansky, P. Selles, and L. Malegat, Phys. Rev. A **68**, 052701 (2003).
[20] C. Bouri, P. Selles, L. Malegat, J. M. Teuler, M. Kwato Njock, and A. K. Kazansky, Phys. Rev. A **72**, 042716 (2005); C. Bouri, P. Selles, L. Malegat, and M. G. Kwato Njock, *ibid.* **73**, 022724 (2006).
[21] L. Feng and H. W. van der Hart, Phys. Rev. A **66**, 031402(R) (2002).
[22] L. Feng and H. W. van der Hart, J. Phys. B **36**, L1 (2003).
[23] C. W. McCurdy, D. A. Horner, T. N. Rescigno, and F. Martín, Phys. Rev. A **69**, 032707 (2004).
[24] B. Fornberg and D. M. Sloan, Acta Numerica 203 (1994).
[25] E. S. Smyth, J. S. Parker, and K. T. Taylor, Comput. Phys. Commun. **114**, 1 (1998); J. S. Parker, L. R. Moore, K. J. Meharg, D. Dundas, and K. T. Taylor, J. Phys. B **34**, L69 (2001).
[26] J. Colgan, M. S. Pindzola, and F. Robicheaux, J. Phys. B **34**, L457 (2001).
[27] J. Colgan and M. S. Pindzola, Phys. Rev. A **65**, 032729 (2002); Phys. Rev. Lett. **88**, 173002 (2002).
[28] S. X. Hu, J. Colgan, and L. A. Collins, J. Phys. B **38**, L35 (2005).
[29] U. Kleiman, J. Colgan, M. S. Pindzola, and F. Robicheaux, in *Proceedings of the International Conference on Electron and Photon Impact Ionization and Related Topics, Louvain-la-Neuve, Belgium, 2004*, edited by B. Piraux, IOP Conf. Ser. No. 183 (Institute of Physics, Bristol, 2005), p. 131.
[30] S. Laulan and H. Bachau, in *Proceedings of the International Conference on Electron and Photon Impact Ionization and Related Topics, Metz, France 2002*, edited by L. U. Ancarani, IOP Conf. Ser. No. 172 (Institute of Physics, Bristol, 2003), p. 109.
[31] S. Laulan and H. Bachau, Phys. Rev. A **69**, 033408 (2004).
[32] H. Bachau, E. Cormier, P. Decleva, J. E. Hansen, and F. Martín, Rep. Prog. Phys. **64**, 1815 (2001).
[33] S. Laulan and H. Bachau, Phys. Rev. A **68**, 013409 (2003).
[34] B. Piraux and G. Lagmago Kamta, in *Proceedings of the NATO Advanced Research Workshop on Super-Intense Laser-Atom Physics, Han-sur-Lesse, Belgium, 2000*, edited by B. Piraux and K. Rzażewski, Vol. 12 of *NATO Science Series II: Mathematics, Physics and Chemistry* (Kluwer Academic, Dordrecht, 2001), p. 127.
[35] S. Laulan, H. Bachau, B. Piraux, J. Bauer, and G. Lagmago Kamta, J. Mod. Opt. **50**, 353 (2003).
[36] G. Lagmago Kamta, B. Piraux, and A. Scrinzi, Phys. Rev. A **63**, 040502(R) (2001).
[37] B. Piraux, J. Bauer, S. Laulan, and H. Bachau, Eur. Phys. J. D **26**, 7 (2003).
[38] E. J. Heller and H. A. Yamani, Phys. Rev. A **9**, 1201 (1974).
[39] B. A. Finlayson, *The Method of Weighted Residuals and Variational Principles* (Academic Press, New York, 1972).
[40] See, e.g., A. K. Bhatia and A. Temkin, Rev. Mod. Phys. **36**, 1050 (1964); J. S. Sims and W. C. Martin, Phys. Rev. A **37**, 2259 (1988); A. Scrinzi and B. Piraux, *ibid.* **56**, R13 (1997).
[41] C. L. Pekeris, Phys. Rev. **112**, 1649 (1958).
[42] M. Rotenberg, Adv. At. Mol. Phys. **6**, 233 (1970).
[43] E. Huens, B. Piraux, A. Bugacov, and M. Gajda, Phys. Rev. A **55**, 2132 (1997).
[44] B. Grémaud and D. Delande, Europhys. Lett. **40**, 363 (1997).
[45] D. A. Varshalovich, A. N. Moskalev, and V. K. Khersonskii, *Quantum Theory of Angular Momentum* (World Scientific, Singapore, 1988).
[46] A. W. Weiss, Phys. Rev. **122**, 1826 (1961).
[47] J. T. Broad, Phys. Rev. A **31**, 1494 (1985).
[48] C. C. J. Roothaan and A. W. Weiss, Rev. Mod. Phys. **32**, 194 (1960).
[49] M-K. Chen, J. Phys. B **26**, 3025 (1993).
[50] M. Masili, J. J. De Groote, and J. E. Hornos, J. Phys. B **33**, 2641 (2000).
[51] G. W. F. Drake, Phys. Rev. Lett. **65**, 2769 (1990); G. W. F. Drake and Z-C. Yan, Phys. Rev. A **46**, 2378 (1992).
[52] A. Bürgers, D. Wintgen, and J-M. Rost, J. Phys. B **28**, 3163 (1995).
[53] S. P. Goldman, Phys. Rev. Lett. **73**, 2547 (1994); Phys. Rev. A **52**, 3718 (1995).
[54] This relation does not mean that the parity of a given state depends on the total angular momentum L. In fact, this relation defines the parity of the states that are actually coupled by the dipole interaction Hamiltonian.
[55] R. Shakeshaft, Phys. Rev. A **34**, 244 (1986).
[56] *Handbook of Mathematical Functions*, edited by M. Abramowitz and I. A. Stegun (Dover, New York, 1972).
[57] G. H. Golub and C. F. Van Loan, *Matrix Computations*, 3rd ed. (Johns Hopkins University Press, Baltimore, 1996).
[58] T. Li and R. Shakeshaft, Phys. Rev. A **71**, 052505 (2005).

[59] G. W. F. Drake, Nucl. Instrum. Methods Phys. Res. B **31**, 7 (1988).
[60] M. Venuti and P. Decleva, J. Phys. B **30**, 4839 (1997).
[61] J. T. Broad and W. P. Reinhardt, J. Phys. B **9**, 1491 (1976).
[62] J. T. Broad and W. P. Reinhardt, Phys. Rev. A **14**, 2159 (1976); R. Gersbacher and J. T. Broad, J. Phys. B **23**, 365 (1990).
[63] H. R. Sadeghpour, C. H. Greene, and M. Cavagnero, Phys. Rev. A **45**, 1587 (1992).
[64] M. Gailitis and R. Damburg, Proc. Phys. Soc. London **82**, 192 (1963).
[65] V. I. Kukulin, V. M. Krasnopol'sky, and J. Horáček, *Theory of Resonances, Principles and Applications*, Reidel Texts in the Mathematical Sciences (Kluwer Academic, Dordrecht, 1989), p. 306.
[66] W. Vanroose, J. Broeckhove, and Fr. Arickx, Phys. Rev. Lett. **88**, 010404 (2002).
[67] A. Kheifets, J. Phys. B **34**, L247 (2001).
[68] D. Proulx and R. Shakeshaft, J. Phys. B **26**, L7 (1993).
[69] E. Hairer, S. P. Norsett, and G. Wanner, *Solving Ordinary Differential Equations I: Non-stiff problems* (Springer Verlag, Berlin, 1987).
[70] A. Scrinzi and B. Piraux, Phys. Rev. A **58**, 1310 (1998).
[71] H. C. Day, B. Piraux, and R. M. Potvliege, Phys. Rev. A **61**, 031402(R) (2000).
[72] Flat pulses with short turn-on and -off linear ramps have been used by many authors. It is interesting to mention that in this case the kernel is broader as expected, therefore requiring longer pulses to get the same accuracy as for cosine square pulses.
[73] J. A. R. Samson, W. C. Stolte, Z.-X. He, J. N. Cutler, Y. Lu, and R. J. Bartlett, Phys. Rev. A **57**, 1906 (1998).
[74] M. A. Kornberg and J. E. Miraglia, Phys. Rev. A **49**, 5120 (1994).
[75] C. A. Nicolaides, C. Haritos, and T. Mercouris, Phys. Rev. A **55**, 2830 (1997).
[76] M. S. Pindzola and F. Robicheaux, Phys. Rev. A **58**, 4229 (1998).
[77] H. Hasegawa, E. J. Takahashi, Y. Nabekawa, K. L. Ishikawa, and K. Midorikawa, Phys. Rev. A **71**, 023407 (2005).